Teng *et al. Microstructures* 2023;3:2023019
DOI: 10.20517/microstructures.2023.07

Microstructures

Review

Open Access

Filled carbon-nanotube heterostructures: from synthesis to application

Yu Teng[1,2,#], Jing Li[1,#], Jian Yao[1], Lixing Kang[1], Qingwen Li[1]

[1]Advanced Materials Division, Suzhou Institute of Nano-Tech and Nano-Bionics, Chinese Academy of Sciences, Suzhou 215123, Jiangsu, China.
[2]School of Nano Science and Technology, University of Science and Technology of China, Hefei 230026, Anhui, China.
[#]Authors contributed equally.

Correspondence to: Prof. Lixing Kang, Advanced Materials Division, Suzhou Institute of Nano-Tech and Nano-Bionics, Chinese Academy of Sciences, Suzhou 215123, Jiangsu, China. E-mail: lxkang2013@sinano.ac.cn; Prof. Qingwen Li, Advanced Materials Division, Suzhou Institute of Nano-Tech and Nano-Bionics, Chinese Academy of Sciences, Suzhou 215123, Jiangsu, China. E-mail: qwli2007@sinano.ac.cn

How to cite this article: Teng Y, Li J, Yao J, Kang L, Li Q. Filled carbon-nanotube heterostructures: from synthesis to application. *Microstructures* 2023;3:2023019. https://dx.doi.org/10.20517/microstructures.2023.07

Received: 2 Feb 2023 **First Decision:** 14 Mar 2023 **Revised:** 20 Mar 2023 **Accepted:** 23 Mar 2023 **Published:** 3 Apr 2023

Academic Editor: Yang Ren **Copy Editor:** Fangling Lan **Production Editor:** Fangling Lan

Abstract

Carbon nanotubes (CNTs) have a one-dimensional (1D) hollow tubular structure formed by graphene curling with remarkable electronic, optical, mechanical, and thermal properties. Except for the applications based on their intrinsic properties, such as electronic devices, THz sensors, and conductive fiber, CNTs can also act as nano-vessels for nano-chemical reactions and hosts for encapsulating various materials to form heterostructures. In this review, we have summarized the research status on filled carbon-nanotube heterostructures from four aspects: synthesis, morphological and electronic structure analysis, potential applications, and perspective. We begin with an overview of the filling methods and mechanisms of the 1D heterostructures. Following that, we discuss their properties in terms of morphological and electronic structure. The burgeoning applications of 1D heterostructures in nano-electronic, energy, storage, catalysis, and other fields are then thoroughly overviewed. Finally, we offer a brief perspective on the possible opportunities and challenges of filled CNTs heterostructures.

Keywords: Filled carbon nanotubes heterostructures, confinement effect, morphological structure, electronic structure, applications

INTRODUCTION

CNTs have received widespread attention since they were confirmed to exist in 1991 by Japanese scientist Iijima[1] due to their one-dimensional (1D) nanostructure with remarkable electronic[2], optical[3], mechanical[4], and thermal properties[5]. Because of these characteristics, CNTs are critical for the advancement of electronics and nanoelectronics[6]. For single-walled carbon nanotubes (SWCNTs), the nanotube band structure is determined by the nanotube radius and chirality, which can be either metallic or semiconductor[7]. Using a SWCNT as the gate and molybdenum disulfide (MoS_2) as channel materials, a one-nanometer physical gate length transistor with a subthreshold swing of ~65 mV dev^{-1} at 298 K was achieved, breaking the five-nanometer-limitation of Si technology[8]. Furthermore, as separation methods for high-purity semiconductor single-walled carbon nanotube (s-SWCNT, > 99.99%)[9] have matured, high-performance high-density arrays s-SWCNT field effect transistors have been developed[10], positioning s-SWCNTs as the candidate elements for the manufacture of next-generation electronic devices.

Another intriguing feature of CNT is its unusual tubular structure with a nanometer diameter, which makes it an ideal nanoscale vessel for restricted chemical reactions[11] as well as a powerful method to control the electronic structure of CNTs by filling it with specific substances[12]. Since the feasibility of filling carbon nanotubes with guest substances was predicted in 1992, and the Pb@MWCNT was first synthesized in 1993[13], attempts to fill the CNTs with gas, liquid, and solid substances have been extensively explored. According to the aforementioned pioneering works, numerous new nanoclusters[14], nanowires[15], and nanoribbons guests[16] were observed inside CNTs, which were different from that in their bulk states[17] due to the confined space of 1D nanotube channels. To exhibit the influence of the diameter of the CNTs, SnTe nanowires, for example, were transformed from monatomic chains to curvilinear chains, hyperbolic chains, and then to 2 × 2 rock salt[18]. CNT template-assisted growth can help produce 1D materials with high aspect ratios. However, nanoscale materials are thermodynamically unstable and susceptible to degradation by air and water. Materials encapsulated within CNTs can be protected from reactions with the surrounding medium, particularly oxidation, when exposed to air. Additionally, nanoscale guest materials within CNTs can be stabilized by the strong carbon walls acting as a barrier. In a highly confined space, X@CNTs provide a new combination to strengthen and stabilize chemical elements, enabling chemically stable new crystal structures[19]. As a result, the filled carbon-nanotube heterostructures pave the way for research into confinement-stabilized nonequilibrium materials and related emergent physical phenomena.

On the other hand, the carbon nanotube's electronic band structure would be modified by the interaction between the carbon wall and the guest substance[12,20]. Synthesized SWCNT samples consist of a mixture of metallic and semiconducting nanotubes, resulting in uneven properties. Customizing the electronic properties of SWCNTs is crucial for their advanced applications. Therefore, filling CNTs to control their electronic structure is necessary. For strongly interacting heterostructure systems, allowing for electron exchange between the encapsulated electron donor or electron acceptor materials and the CNTs, which controls the electronic properties of CNTs. For instance, the electronic acceptor 1,1′-didodecyl-4,4′-bipyridinium dihexafluorophosphate (Viol) was filled into the metallic SWCNT to transit it into the semiconducting state[21]. For weakly interacting heterostructure systems, although the electron transfer is hindered, the radial vibrations of the carbon nanotubes are suppressed, causing them to deform[22]. The single CNT in discrete-filled heterostructure systems would split into a series of quantum dots[23]. Therefore, CNTs can be designed with the help of filling for particular applications, such as sensors[24], p-n junctions[25], transistors[26] and so forth.

The purpose of this manuscript is to give an overview of the state-of-the-art research on filled CNTs heterostructures, from synthesis to application. The filling methods and mechanism are covered in detail in

the Section "INTRODUCTION" of the review. The investigation of the morphological and electronic structure of filled CNTs heterostructures using transmission electron microscopy and spectroscopic techniques forms the focus of the Section "FILLING METHOD AND MECHANISM" of the review. The Section "MORPHOLOGICAL AND ELECTRONIC STRUCTURE OF FILLED CNTS HETEROSTRUCTURES" of the manuscript reviews potential applications of filled CNTs heterostructures in a different field. Finally, we put forward a view on the possible opportunities and challenges of filled CNTs heterostructures.

FILLING METHOD AND MECHANISM

Successful filling of gas, liquid, and solid materials into the hollow nanospace of the CNT is possible, and the filling methods are categorized as *in situ* (filling of CNT during their growth)[27] and *ex-situ* (filling of pre-formed CNT)[28]. The mechanism of filling materials inside CNTs is mainly due to the unique tubular structure of CNTs, which provides a sealed space for encapsulating materials inside. The diameter of CNTs can be controlled to match the size of guest molecules, thereby effectively trapping them inside. In addition, the strong van der Waals force between guest molecules and the inner wall of CNTs also helps to limit the effect and prevent molecules from diffusing outward. Depending on the properties of the filled materials, the vast majority of filled CNTs heterostructures are made using the *ex-situ* method, which primarily includes encapsulation from the gas or liquid phases, as well as sequential transformations in the cavity after pre-encapsulation. According to some studies, the adsorption effect of the lumens of carbon nanotubes is the main reason for filling the gas molecule[29]. The principle of filling liquids and solids is mainly based on capillary and wetting effects[30]. According to Young's equation and Laplace equation theory, the force between the liquid and the inner surface of the carbon tube must be large enough to allow it to infiltrate[31]. During the filling process, it is inevitable that the CNTs will have indirect contact or a surface coating with the guest material, and necessary post-processing, such as cleaning with appropriate solvents, is required to maximize the elimination of residual substances outside the tube that may affect the system.

In-situ filling

In-situ filling is filling CNTs directly with foreign material while they are being synthesized. As a result, the carbon nanotubes can be kept intact with a high fill rate, effectively isolating the encapsulation material from the surrounding environment. However, the *in situ* filling method yields a low filling yield, and some impurity elements will enter the interior of the carbon nanotubes during the filling process[32]. *In situ* filling mainly includes arc discharge[33] and molten salt electrolysis[34].

The arc discharge method is also called the graphite arc method. The vacuum reactor is filled with inert gas or hydrogen. Graphite rods of different sizes are used as electrodes. During the growth and filling process, the graphite rods at one end are gradually consumed, and the carbon nanotubes grow at the other end. This method was used by Guerret-Piécourt *et al.* to create element-filled CNTs *in situ*[33].

Molten salt electrolysis is a method in which an inorganic salt is heated to melt into a liquid electrolyte in a carbon crucible for electrolysis to fill CNTs, which was first proposed by Hsu *et al.* They used this method to fill CNTs with Li_2C_2, LiCl, Sn, Pb, Bi, and Sn-Pb alloy[34,35].

Ex-situ filling

Ex-situ filling refers to the process of filling guest substances into the pre-synthesized carbon nanotubes, which is the most widely used approach to filled nanotubes preparation. According to the physical properties of the filled materials, they are introduced into the cavity of CNTs in the form of liquid or steam, corresponding to the liquid phase method and the gas phase method[28], respectively. In order to fill the

CNTs, their ends need to be opened first. Heat treatment in an oxidizing environment, such as H_2O_2, O_2[36], O_3[37], HNO_3, H_2SO_4[38], $KMnO_4$[39], or Br_2[40] is mainly used opening approaches. To obtain a more pure CNT, combined thermal treatment and concentrated acid treatment are necessary to remove the various contaminants, such as amorphous carbon, graphite electrode particles, and catalyst[41].

Filling of CNTs from the liquid phase entails impregnating the opened tube with melts or solutions of target compounds. Although many examples of liquid-phase filling of carbon nanotubes have been reported, the mechanism has not been determined. We assume that liquid-phase filling of carbon nanotubes is a so-called capillary wetting phenomenon[30], then the Young and Laplace equations can be used to describe the mechanism[31]:

$$\Delta P_{re} = \beta \cdot \frac{R + r}{R \cdot r} \tag{1}$$

where ΔP_{re} represents the pressure change, β represents the surface tension coefficient, and R and r represent two different curvature radii of the surface, respectively. When the liquid level in the nanotube rises, it saturates the tube wall and forms a meniscus at the top [Figure 1].

The meniscus is approximately regarded as a spherical shape, and the liquid is in contact with the capillary wall at a certain angle θ, then the following formula is obtained[31]:

$$\Delta \rho = \frac{2\beta cos\theta}{r} \tag{2}$$

where $\Delta\rho$ is the density difference between two phases.

According to the equation, when the contact Angle exceeds 90°, external forces are needed to drive the rise of capillarity. When the contact angle is below 90°, spontaneous filling will occur. Surface tension β is the force of liquid surface shrinkage. Liquids with low surface tension are more likely to spread through the tube, which is manifested by the smaller contact angle and the reduced driving force required for spontaneous filling. β of some common solvents and metal halides packed into carbon nanotubes at the melting point has been tested or calculated as follows (unit: mN/m): water (72.8), methanol (22.07), acetone (23.46), tetrachloromethane (26.43)[42], AgCl (113-173), AgBr (151), AgI (171), KCl (93), KI (70), $NdCl_3$ (102), $ZnCl_4$ (1.3), PbO (132), V_2O_5 (53), *etc.*[43] The filling of salts such as metal halides and oxides is often carried out in this method, such as KI, AgI, and Sb_2O_3 filled by Sloan's group[44]. The following table[45-66] is a list of various materials that have been reported in the literature for filling CNTs in recent years.

Vacuum and high temperatures are used to fill CNTs from the gas phase. An encapsulated material is heated inside a sealed tube until it vaporizes (or sublimates), but keep the temperatures as low as possible to prevent (or reduce) de-encapsulation[35]. The vapor of the compound that is enclosed during CNTs annealing enters the nanotube via capillary condensation and crystalizes during subsequent cooling. During the gas phase filling process, no other substances are introduced; thus, there is no pollution to the environment[67]. The major defect of this approach, however, is also obvious. First, the reaction temperature should be less than 1,000 °C to avoid destroying the CNTs or reacting with carbon to close the CNT's ends[67]. Second, the filled substances are typically discrete in the hollow nanospace of CNTs, which makes it difficult to control the filling yields[68]. As a result, the gas phase filling approach is appropriate for molecule crystals containing inorganic clusters, organic molecules, and complexes with low boiling or sublimation temperatures. The filling systems for fullerenes[61] and their derivatives[69] are typical examples.

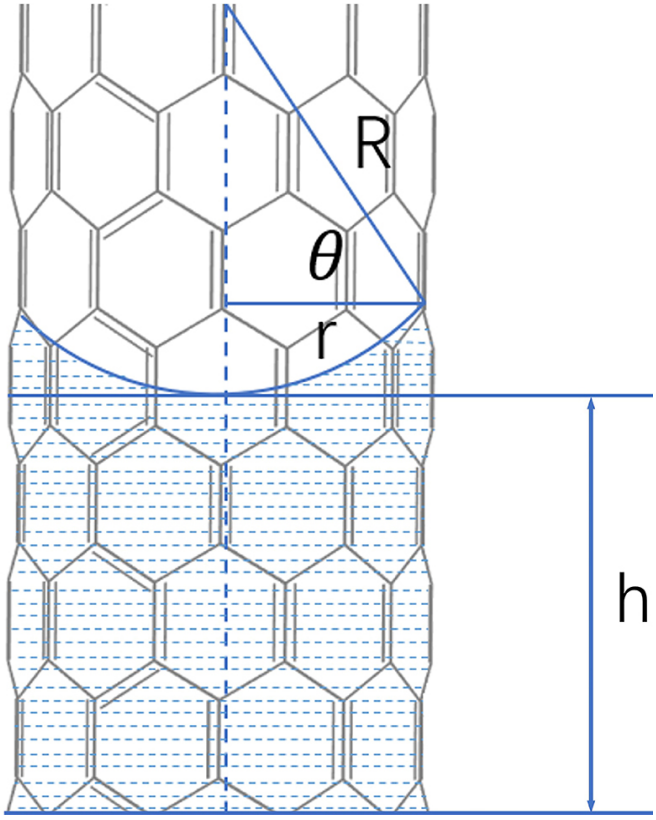

Figure 1. The liquid level rises in a capillary.

Recently, a novel method for multistep inorganic synthesis has been established, in which the pre-filled nanotube undergoes sequential chemical transformations[70]. For example, the metal precursors, such as metal halides and complexes, are first pre-filled into the CNTs and then perform thermal decomposition or Hydrogen reduction to form metal nanoparticles@CNT. After that, the second reactant, such as H_2S, Te, is introduced and reacted with the metal nanoparticles to yield chalcogenides. For example, inorganic nanoribbons $[MS_2]_n$@SWCNT (M = Mo or W) can be prepared through sequential transformations of $M(CO)_6$ (M = Mo or W) to nanoclusters and nanoclusters to nanoribbons [Figure 2A]. Various graphene nanoribbons can be obtained by high-temperature polymerization of the selected small organic molecules encapsulated in the cavities of CNTs [Figure 2B][16].

MORPHOLOGICAL AND ELECTRONIC STRUCTURE OF FILLED CNTS HETEROSTRUCTURES

The characteristics of CNTs mainly include hollow nanospace morphology[71], conductivity, chirality[72], and so on. Two critical questions must be addressed as the substance fills the carbon tube. First, how does the coaction between the inner filler and the carbon tube modify the characters of the carbon tube itself? Second, how does the confined space of the carbon tube affect the crystal phase and heterostructures of the inner filler? The former has significant implications for the application of the new heterostructures, whereas the latter can be used to study many space-confined scientific issues. Therefore, this section discusses the morphological and electronic structure of some intriguingly filled CNTs heterostructures.

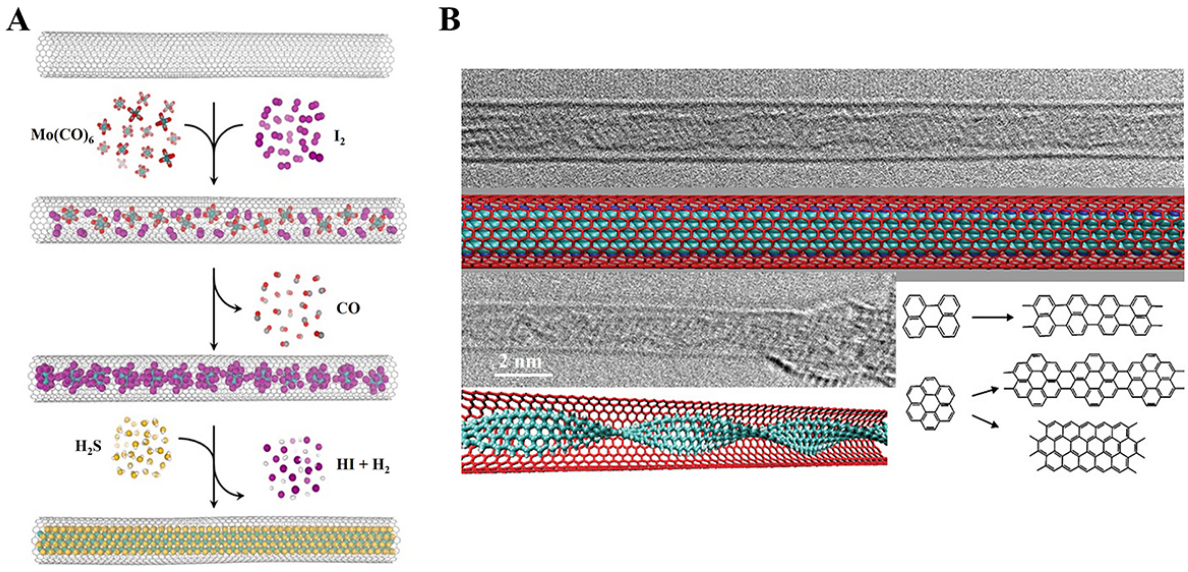

Figure 2. Multistep synthesis performed in carbon nanotubes: (A) Multistep in organic synthesis. The encapsulation and conversion of $Mo(CO)_6$ and iodine molecules into $[Mo_6I_{14}]^{2-}$ nanocluster and regenerate $[MoS_2]_n$ nanoribbons (Reproduced with permission[70]. Copyright 2016, American Chemical Society). (B) Multistep organic synthesis. The encapsulation and conversion of the organic molecule perylene or coronene into graphene nanoribbons (Reproduced with permission[16].Copyright 2011, American Chemical Society).

Morphological structure of filled CNTs heterostructures

As mentioned in Table 1, various inorganic as well as organic materials have been filled in the CNTs until today. To study the morphological structure of the heterostructures, transmission electron microscopy (TEM) is a basic research method. Studies have shown that when the accelerating voltage of TEM is less than 86 kV, the carbon nanotubes can still maintain structural integrity under the action of high-energy electron beams[73]. High-resolution transmission electron microscopy (HR-TEM) provides clearer internal structure information than TEM, such as interplanar spacing, atomic arrangement, and other information[74]. HR-TEM allows researchers to directly "observe" chemical reactions in nanoscale space. Aberration-corrected transmission electron microscopy (AC-TEM) is more powerful than HR-TEM in structure information. The biggest advantage of AC-TEM is that spherical aberration correction reduces aberration and thus improves resolution. The resolution of traditional TEM is at the nanometer scale, while the resolution of AC-TEM can reach the Å scale[75]. Improved resolution means a deeper understanding of the material, making observations of single atoms possible. Here, we attempt to provide a brief review of the previous efforts made in the compounding of X@CNTs based on the chemical composition of the filling objects.

Element materials

Element materials with low sublimation temperatures can be filled using the gas phase method by placing opened CNTs and bulk powder under a high vacuum and high temperature directly. Guan *et al.* introduced iodine to SWCNTs by heating the opened SWCNT and iodine elemental in a clean glass tube [Figure 3A][76]. The structure of the filled iodine transitions from the helical atomic chain to the crystalline phase as the diameter of the SWCNT becomes larger from Figure 3B. Phase transitions of I from chains to crystalline structures are observed inside the SWCNT around the critical diameter of 1.45 ± 0.05 nm. Furthermore, the structure of the host SWCNT is elliptically distorted by the helical I_n chains because of the repulsive interaction between I_3^- or I_5^- species and the SWCNT. In the Te@SWCNT system, the single-chain or few-chain limit Te nanowire also exhibits a helical structure, but the behavior maintains the structural

Table 1. Various materials for filling CNTs

Material	CNT	Method	Outcomes	Applications	Ref.
Sn	MWCNTs	Arc discharge	Enhance microwave absorption.	Microwave absorbent	[45]
S	SWCNTs/DWCNTs	CVT	Self-assembly of conductive sulfur chains in CNTs is realized.		[46]
Te	DWCNTs	CVT	Observe the Raman response of tellurium-filled CNTs.	Optoelectronic devices	[47]
Eu	SWCNTs	CVT	A high yield controlled synthesis method for Eu nanowires is proposed.	Electronic devices	[48]
GaTe/SnS/Bi_2Se_3	SWCNTs	CVT	GaTe, SnS, and Bi_2Se_3 are encapsulated into the SWCNTs for the first time.	Electronic devices	[49]
Nb/V/$TiTe_3$	MWCNTs	CVT	MTe_3 are synthesized in CNTs for the first time.		[50]
$NbSe_3$	MWCNTs	In-tube reaction	A single nanowire $NbSe_3$ is synthesized for the first time.		[51]
Bi_2Te_3/GaSe	SWCNTs	In-tube reaction	Bi_2Te_3 and GaSe are encapsulated into the SWCNTs for the first time.	Electronic devices	[52]
$CsPbBr_3$/$CsSnI_3$	SWCNTs	In-tube reaction	The smallest isolated halide perovskite structure is synthesized within CNTs.	Optoelectronic devices	[53]
Fe-S	CNTs	CVT	Fe-S@CNTs are prepared using CNT as a reactor.	Anode material	[54]
CdSe	SWCNTs	In-tube reaction	CdSe nanowires are prepared by self-assembly and directional assembly under the constraint of SWCNTs.	Optoelectronic devices	[55]
ReS_2	SWCNTs	In-tube reaction	Ultrathin ReS_2 nanoribbons are synthesized for the first time.	Nano-electrodes	[56]
$HfTe_2$	CNTs	In-tube reaction	$HfTe_2$ nanoribbons are synthesized by CVT in CNTs.	Metal-semiconductor Schottky heterojunctions	[57]
WS_2	SWCNTs/ DWCNTs	In-tube reaction	WS_2 nanoribbons with uniform widths are synthesized using CNTs as templates.	Spintronics	[58]
SnSe	SWCNTs	CVT	It is demonstrated that SnSe form ordered nanocrystals in narrow SWCNTs, and the band gap is significantly enlarged.	Solar cells	[59]
MoS_2	SWCNTs/DWCNTs	In-tube reaction	MoS_2 nanoribbons with uniform width are synthesized using CNTs as a template.	Synthesis method	[60]
C_{60}	SWCNTs	CVT	The relationship between electron dose and the bimolecular reaction of fullerene in CNTs is reported.		[61]
N@C_{60}	SWCNTs	CVT	N@C_{60}@SWCNTs are synthesized, and it was found that pod samples could be converted into DWCNTs.		[62]
Gd@C_{82}	MWCNTs	CVT	The transport characteristics of Gd@C_{82}@CNTs as a field effect transistor channel are introduced.	Electronic devices	[63]
Sc_3N@C_{80}	SWCNTs	CVT	Nano-pods formed by Sc_3N@C_{80} are prepared and characterized.		[64]
La@C_{82}	SWCNTs	CVT	EELS is used to measure the charge transfer between materials.		[65]
Gd_2@C_{92}	SWCNTs	CVT	The dynamic behavior of limit atoms in metallic fullerenes is observed by HRTEM		[66]

MWCNTs: Multi-walled carbon nanotubes; DWCNTs: double-walled carbon nanotubes; CVT: chemical vapor transport; EELS: electron energy loss spectroscopy; HRTEM: high-resolution transmission electron microscopy.

characteristics of Te nanowire crystal rather than the interaction between Te and CNT [Figure 3C][77]. However, the situation became more complicated for element S of the same group as Te after being filled. It was observed that the sulfur chains confined within the carbon nanotubes lacked a definite structure[78] and were markedly different from the previously proposed linear or zigzag structures[46]. Instead, they tended to assume conformations resembling the cyclo-S_8 allotrope. Density functional theory (DFT) calculations showed that a more disordered sulfur chain structure was more stable than linear and zigzag conformations when the sulfur chain was confined within the SWCNT. Various nanowires, such as Eu [Figure 3D][48] and Sn [Figure 3E][15], are filled in carbon nanotubes using this simple process.

For element materials with high melting point temperatures or strong chemical active and unstable, multistep sequential chemical transformations within the pre-filled nanotube is an effective method. Novel metal nanowires (Ag[79], Pt[80], *etc.*), 3d metal (Fe[81], Co[82], Ni[83] *etc.*), and carbon nanowires[84] filled inside CNT were synthesized with this method. For example, the nanowire Fe, Co, Ni, and their alloys@CNTs can be synthesized by the pyrolysis of related pre-filled metallocene@CNT. The Fe nanowire filled inside CNT has a diameter of 20-40 nm with a filling of 60% and exhibits strong ferromagnetic behavior at room temperature[85]. Similarly, the ferromagnetic nanowires filled CNTs with different reaction precursors were also reported in several other pieces of literature[86]. As a true 1D nanocarbon, the sp^1 hybridized carbon chain is predicted to have novel chemical and physics properties, but because of its strong chemical activity and extreme instability, it is difficult to synthesize in common conditions[87]. In 2016, the sp^1 hybridized carbon chain inside DWCNTs (LLCC@DWCNT) was first synthesized by Shi *et al.*, which provides a practical strategy for the preparation of the true 1D carbon chain [Figure 3F][84].

Organic and metal-organic molecule cluster

The vast majority of organic molecules are nanosized but less stable in the atmospheric environment[88]. Filling the molecule inside the cavity of CNT can improve molecular stability while also serving as a precursor for the preparation of other complex materials, such as graphene nanoribbons[16], polymers compounds[89], and inorganic metal compounds[14].

C_{60} was the first molecule studied inside CNTs[90]. Following that, many other larger fullerenes[91] and endohedral metallofullerenes[92] were successfully filled and were used to study the interaction, intermolecular spacing, molecular orientation, molecular motion, and reaction behavior in the confined space. According to TEM measurements of C_{60}@CNTs, the intermolecular spacing in the nanotube is shorter than in bulk crystals, which is coincident with the van der Waals forces that induce compression of fullerenes inside the nanotube [Figure 4A][61]. The stacking mode of C_{60} in CNTs is sensitive to nanotubes' internal diameters, demonstrating the confinement effect inside nanotubes. C_{60}@SWCNTs is relatively stable below 800 °C in the vacuum state of less than 1×10^{-6} Torr, whereas fullerenes in nanotubes gradually polymerize above 1,000 ℃ or under the electron beam. A series of intermediate structures, such as a dimer, trimer, and chain, gradually transform to form complete nanotubes. Endohedral metallofullerenes have electric dipole moments caused by metal atoms within the carbon cage, which can affect their behavior inside nanotubes. Using Ce@C_{82} as a model molecule, the influence of the dipolar interactions on molecular orientations in CNTs was investigated by using HR-TEM[93] [Figure 4B]. The molecules have a tendency to align their dipolar moments along the nanotube axis, enhancing electrostatic interactions between nearby molecules, which does not occur in Ce@C_{82} crystals or solutions.

Because of the exact geometrical match between fullerene and the interior of a nanotube, some globular non-fullerene molecules, such as o-carborane[94], octasiloxane [Figure 4C][95], metal-organic cluster[14], polyoxometalates (POM) [Figure 4D][89], were also tried to fill inside the CNTs. Because it has a smaller

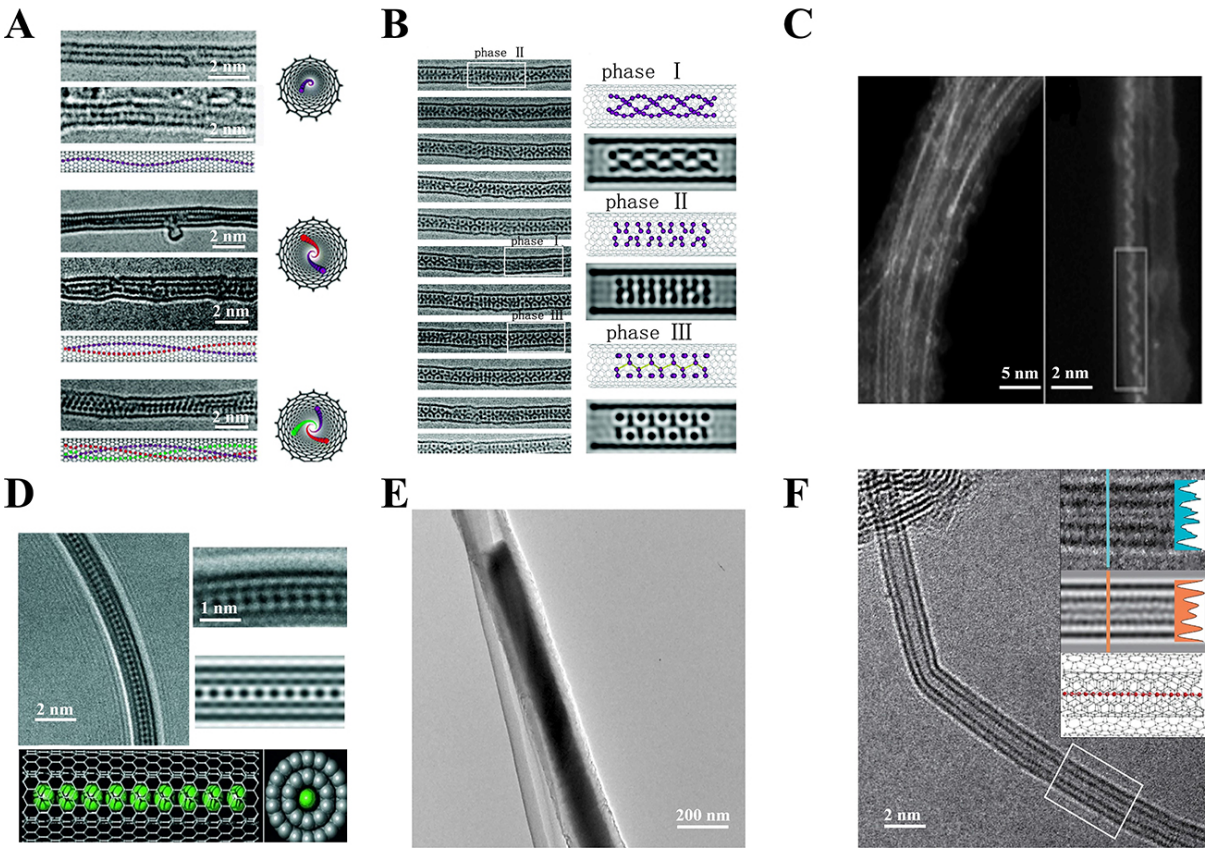

Figure 3. Elemental filling examples: (A) HR-TEM images and schematic illustrations of the chains of iodine filled in SWCNTs (Reproduced with permission[76]. Copyright 2007, American Chemical Society). (B) The phase transition of iodine from atomic chains to crystalline structures (Reproduced with permission[76]. Copyright 2007, American Chemical Society). (C) High magnifying STEM ADF image of Te-filled CNTs (Reproduced with permission[77]. Copyright 2020, Springer Nature). (D) HR-TEM image and simulated diagram of Eu's single chain filled in DWCNTs (Reproduced with permission[48]. Copyright 2009, Wiley). (E) TEM image of Sn nanowire formed in CNTs (Reproduced with permission[15]. Copyright 2016, Elsevier). (F) LLCC@DWCNT Partial HRTEM images of heterogeneous structures. Inset: a magnified portion of heterostructure (top), a simulated HR-TEM image (middle), and a molecular model (bottom) (Reproduced with permission[84]. Copyright 2016, Springer Nature).

diameter than C_{60}, octasiloxane can enter narrower CNTs than fullerenes[95]. The octasiloxane produces a zigzag packing in the SWCNT, with h-atoms in the corner of the cube in direct contact with the inner surface. In the POM@SWCNT heterostructure, electrons were transferred from SWCNTs to POM clusters, and hybrid materials formed spontaneously in an aqueous solution. Furthermore, many functional metal-organic clusters were also filled inside the CNTs to investigate new nanodevices, such as a spin valve[96] or memory device[97].

Except for the globular molecules, plane molecules can also be filled into the cavity of CNTs. For example, encapsulation of organic salt 1,1′-didodecyl-4,4′-bipyridinium dihexafluorophosphate (Viol) into metallic SWCNTs results in the formation of a semiconductor by opening the band gap [Figure 4E][21]. Small organic molecules, such as perylene and coronene-filled CNTs[16], are used as precursors to produce graphene nanoribbons by high-temperature polymerization.

Metallic inorganic compounds

Varied metallic compounds containing oxides, carbides[98], halides[99], and chalcogenides[100] have been encapsulated inside CNTs using different filling techniques. Many published reviews have discussed

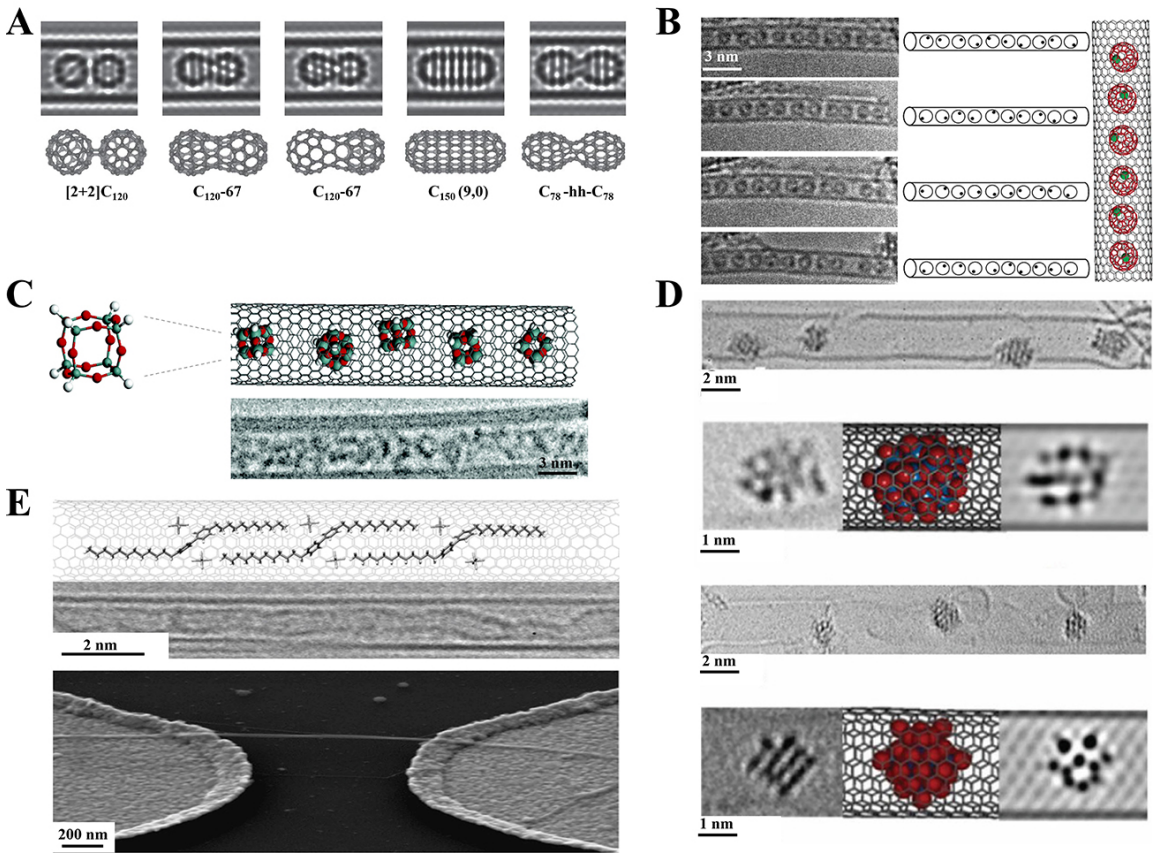

Figure 4. Organic compounds filling: (A) A series of high-resolution images of C_{60} molecules gradually bonded (Reproduced with permission[61]. Copyright 2010, Springer Nature). (B) A series of successive HRTEM images of (Ce@C_{82})@SWCNT and their schematic representation (Reproduced with permission[93]. Copyright 2004, Wiley). (C) Structural diagram of octasiloxane $Si_8H_8O_{12}$; HRTEM micrograph and structural diagram of $Si_8H_8O_{12}$@SWCNT (Reproduced with permission[95]. Copyright 2005, American Chemical Society). (D) AC-HRTEM and simulated images of @SWCNT and {W_{12}}@SWCNT, respectively (Reproduced with permission[89]. Copyright 2019, Wiley). (E) Model illustration of Viol inside a metallic SWCNT, representative AC-HRTEM image of Viol@SWCNT and SEM image of a Viol@SWCNT (Reproduced with permission[21]. Copyright 2017, Wiley).

previously studied examples such as metal oxide[44,101], carbides[61,84], and halides[102-104]. This section will concentrate on some novel structures and systems, such as transition metal dichalcogenides (TMDs)[18,50,56,57,70,101,105-108] and perovskite[53].

Many materials, which are hard to stabilize under normal conditions, form new phases with unique coordination properties in the lumen of CNTs. Under high temperatures, a PbI_2 SWCNT with a diameter ranging from ~3 to 7 nm is first realized inside the hollow nanospace of MWCNT [Figure 5A][109]. The SWCNTs are expected to be steady in the absence of carbon atom protection, and their electronic structure is diameter independent. Recently, Kashtiban *et al.* reported the formation of four isolated halide perovskite nanowires inside ~1.2-1.6 nm SWCNTs via melt insertion of $CsPbBr_3$ and $CsSnI_3$ [Figure 5B][53]. One of the four nanowires has a perovskite-like lamellar structure with polyhedral Sn_4Ix layers, while the other three are ABX_3 perovskite archetypes. Vasylenko *et al.* created SnTe nanowires that filled in CNTs with monatomic, curvilinear chains, hyperbolic chains, and 2 × 2 rock structures by varying the diameter of the CNTs[18]. The study of halide perovskite nanowires and SnTe nanowires filled in CNTs revealed that the structure of the internal filling can be manipulated to design its electronic behavior by changing the diameter of the CNTs.

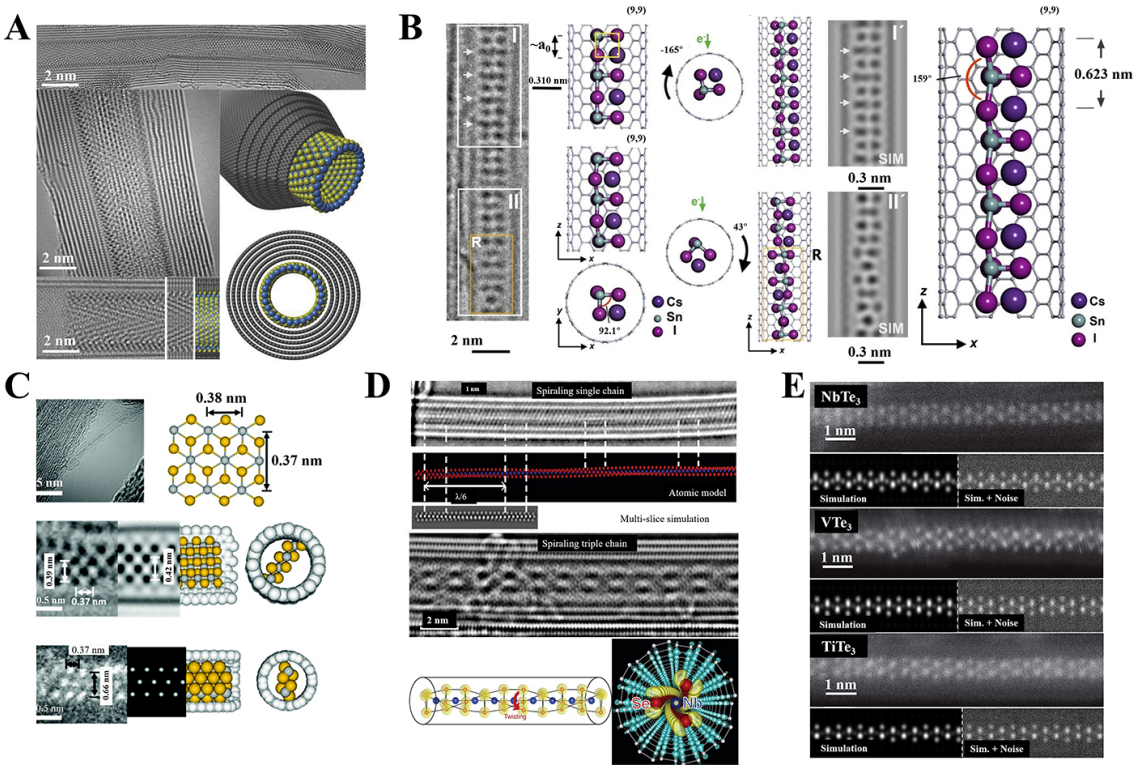

Figure 5. Compounds filling: (A) ACTEM analysis and schematic representation of the PbI_2@SWCNT. Blue: Pb atoms; yellow: I atoms (Reproduced with permission[109]. Copyright 2013, Wiley). (B) HRTEM image and corresponding simulation image of an encapsulated bilayer $CsSnI_3$ perovskite-like polymeric structure derived from $CsSnI_3$ (Reproduced with permission[53]. Copyright 2023, Wiley). (C) ACTEM photos, crystal structure, and geometric optimization models of PtS_2 (Reproduced with permission[106]. Copyright 2017, The Royal Society of Chemistry). (D) TEM and ACTEM images of $NbSe_3$ single strand in DWCNTs, atomic structure model (red: Se, blue: Nb) (Reproduced with permission[51]. Copyright 2018, The American Association for the Advancement of Science). (E) From top to bottom are the ADF-STEM images of MTe_3 single-stranded carbon nanotubes. Illustration below ADF-STEM: ADF-STEM image simulation (left) with the appropriate microscope condition noise added from the structure calculated by the DFT (right) (Reproduced with permission[50]. Copyright 2021, American Chemical Society).

Spurred by the novel electronic, optical, magnetic, and structural properties of graphene nanoribbons[110], isolating and manipulating ultra-fine nanoribbons of 2D materials (e.g., TMDs) has become popular in recent years. However, ultra-fine nanoribbons are difficult to separate and manipulate and may be highly air-sensitive due to the abundance of suspended bonds on the edges of the nanoribbons[111]. Encapsulation of metastable materials inside small-diameter nanotubes has emerged as a novel approach to creating new quasi-1D nanostructures. Cain *et al.* reported a gas-phase synthesis method for producing ultra-fine TaS_2 nanoribbons in CNTs[107]. The boundary and number of nanoribbons were limited by the diameter of the CNTs. Botos *et al.* prepared $[MS_2]_n$@SWCNT (M = Mo or W, average d_{NT} = 1.4 nm) by sequentially transforming $M(CO)_6$ (M = Mo or W) nanocluster to nanoribbons[70]. Two $[MS_2]_n$ nanoribbons, well-ordered crystalline hexagonal structures with zigzag edges, grow inward from both ends of SWCNTs. The nanoribbon's width is strictly regulated due to the limitation of the nanotube diameter. Furthermore, the nanoribbon is twisted rows in the CNTs due to the edge defect. Similar nanoribbon structures were also exhibited in the WS_2@MWCNT[16], $MnTe_2$@SWCNT[105], ReS_2@SWCNT[56], $HfTe_2$@SWCNT[57], and PtS_2@SWCNT [Figure 5C][106] heterostructures. Surprisingly, Nagata *et al.* prepared single MoTe nanowires using CNT as a template and partially oxidized $MoTe_2$ as a precursor[101]. They propose that the MoO_x oxidizes $MoTe_2$ to MoTe and TeO_2. TEM shows that MoTe nanowires exhibit unusual distortion under the confinement of carbon nanotubes, which may provide the possibility for the application of nanowires.

Another type of novel material is composed of 1D chains that are weakly held together by van der Waals interactions. Transition metal tri chalcogenides MX_3 (TMTs, M = transition metal, X= S, Se, Te) are representative examples that allow unusual ground states and collective mode electronic transport in bulk. It is fascinating to isolate and manipulate quasi-1D bulk materials in the few-chain limit because new physics can be induced by the new degree of low dimensionality. In 2018, Pham *et al.* synthesized the single- or few-chain limit of $NbSe_3$ encapsulated in protective MWCNT cavities [Figure 5D][51]. Static and dynamic charge-induced structural torsional waves observed by TEM are not found in bulk $NbSe_3$. Following that, the few-to-single chain limits of $HfTe_3$[108] in the MWCNT cavity were achieved. They discovered that the typically parallel chains in the $HfTe_3$@MWCNT system spiral around each other once three chains are reached, while at the same time, a short-wavelength trigonal antiprismatic rocking distortion takes place, opening a prominent energy gap. Later, they concentrate on MX_3 family members that are not stable in bulk and have been synthesized in the few to a single-chain limit of MTe_3 (M = Nb, V, Ti) within the nanoconfined cavity of MWCNTs [Figure 5E][50].

Electronic structure of filled CNTs heterostructures

Spectroscopy can energetically analyze the interaction between fillers and carbon nanotubes, allowing for a preliminary understanding of the filling material on the electronic structure[112]. Common types of the spectrum include optical absorption spectroscopy (OAS), Raman spectroscopy, and X-ray absorption spectroscopy (XAS).

Optical absorption spectroscopy (OAS)

Optical absorption spectroscopy (OAS) is an experimental technique that measures the ability of a sample to absorb light at different wavelengths. Since energy states are continuous, a substance can only absorb photons with a specific energy in a continuous spectrum. By measuring the amount of light absorbed by the sample, information about the material's electronic and molecular structure can be determined, resulting in spectral information[113]. OAS is a clear and accurate method to investigate the electronic structure of the filled CNTs heterostructures. The OAS technique also has some limitations. One of the main drawbacks is that it can only provide information on the surface or near-surface of the sample, and it is difficult to obtain information about deeper structures. OAS has been used to characterize $CoBr_2$[114], FeX_2[115], AgX[102], CdX_2[116], ZnX_2, CuX[103] (X = Cl, Br, I), $PrCl_3$[117], $TbCl_3$[118], GaSe[119], GaTe[49], Bi_2Se_3[49], SnTe[120], and Bi_2Te_3[52].

The following takes the four heterostructures systems selected in Figure 6A-D as examples to briefly explain the influence of material filling on SWCNTs. The curve of unfilled SWCNTs has several obvious absorption peaks, and the first two peaks, S1 (E^S_{11}) and S2 (E^S_{22}) are connected with the bandgap transition between Van-Hove singularities in semiconductor SWCNTs[102]. The appearance of the M1 (E^M_{11}) peak at about 1.8 eV is because of the inter-band transition of the first Van-Hove singularity in the metal tube. The last peak around 2.4 eV corresponds to a shift in E^S_{33} semiconductor SWCNTs.

Compared with the original data, the OAS of filled heterostructures changed significantly. The change in the spectrum is caused by the local interaction between the carbon atom and the filling atom, which further proves that the change in the electronic properties of SWCNTs is caused by the filling of the inner channel of the carbon tube[103]. The most significant and common phenomenon after being filled with foreign materials is that the optical transition at E^S_{11} is inhibited or even completely quenched because of a charge transfer between the packed substances and the carbon wall[116]. The direction and path of the charge transfer hinge on the properties of the filled materials. Metal halides usually act as electron acceptors, leading to the depletion of electrons in CNTs[115]. Another obvious feature is that all the peaks move towards the low energy region, which can be explained by the shrinking of the energy gap between Van-Hove

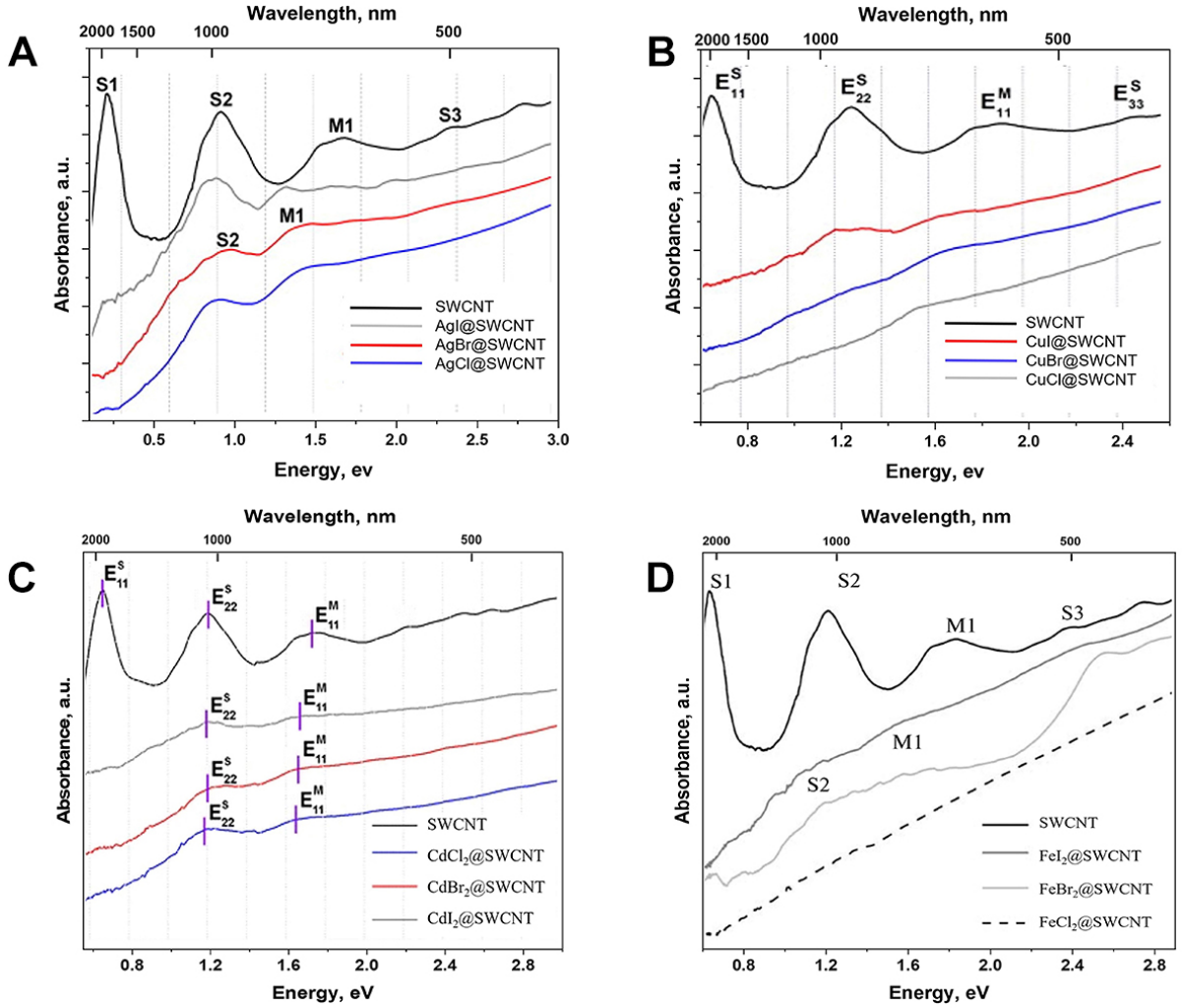

Figure 6. OAS characterization of CNT nanopeapods: (A) OAS of SWCNTs and AgX@SWCNTs (X = Cl, Br, I) (Reproduced with permission[102]. Copyright 2010, Elsevier). (B) OAS of SWCNTs and CuX@SWCNTs (X = Cl, Br, I) (Reproduced with permission[103]. Copyright 2012, Elsevier). (C) OAS of SWCNTs and CdX_2@SWCNTs (X = Cl, Br, I) (Reproduced with permission[116]. Copyright 2013, Springer Nature). (D) OAS of SWCNTs and FeX_2@SWCNTs (X = Cl, Br, I) (Reproduced with permission[115]. Copyright 2009, Springer Nature).

singularities after filling. Notably, the trend of E^S_{22} and E^M_{11} peaks was positively correlated with the electron negativity of halogen atoms (Cl > Br > I)[121]. This phenomenon is most obvious in the CuX@SWCNT and FeX_2@SWCNT systems.

Raman spectroscopy

Raman scattering is a kind of inelastic scattering that occurs when incident light interacts with phonons, and its intensity is typically only one-thousandth of Rayleigh scattering[122]. The energy difference between the scattered light and the incident light can be used to judge the lattice vibration information of carbon nanotubes[122]. Transition metal halide (MX)@CNTs were studied by Raman spectroscopy, such as MnCl, $MnBr_2$[123], $CoBr_2$[114], NiCl, $NiBr_2$[124], ZnCl[104], ZnX_2[104], FeX_2[115], AgX[102], CuX[103] (X = Cl, Br, I), rare earth metal halide, $TbBr_3$, TbI_3[125], $CdCl_2$[126], $LuCl_3$, LuI_3[126], GaSe, GaTe[119], SnS, SnTe[49], Ag[79], Cu, Ni[127], and other complexes.

Kharlamova[123] investigated the $MnCl_2$@SWCNT and $MnBr_2$@SWCNT heterostructures using Raman spectroscopy [Figure 7A and B]. The positions of the RBM peak and G peak of MnX_2 are shifted upward, reflecting the change of carbon-carbon bond energy. It is represented by the change in electronic structure during the filling process. Peak G is shifted in the Raman spectrum of MnX_2@SWCNT, reflecting the charge transfer between the carbon wall and encapsulated materials, which leads to the transition of metallic CNTs to a semiconductor state. The resonance excitation of CNTs of the corresponding diameter can be observed using a laser of specific energy[123]. Metallic SWCNTs with diameters of 1.50 and 1.41 nm were effectively excited at the laser energy of 1.58 eV. The 2.41 eV laser corresponds to a semiconductor SWCNT with a diameter of 1.35 nm. NiX_2@SWCNTs were also studied using Raman spectroscopy [Figure 7C and D]. The peak value of RBM decreased slightly, reflecting the change in CNTs diameter during the filling process. The position of peak G also changed greatly from typical metal nanotubes to semiconductor nanotubes. One possible explanation of the G peak change is that the metal SWCNTs transformed into a semiconductor state after being filled by 1D NiX_2 (X = Cl, Br) nanocrystals; that is, the gap was opened.

The Raman signal enhancement effect is also observed in filled CNTs heterostructure. Nascimento *et al.* reported that the chiral sulfur chains encapsulated in the SWCNTs with a diameter of 0.89 nm can significantly enhance the Raman signal of the SWCNTs[128]. They suggested that the small diameter and hybrid state formed by overlapping orbitals of the sulfur chains and SWCNTs in the excited part of the single-particle electronic spectra are key factors in enhancing the Raman signal. Li *et al.* further discovered that the long polymeric sulfur chains inside HiPco-SWCNTs strongly interact with the sidewalls of the carbon nanotubes, resulting in a decrease in the intensity of the high-frequency Raman spectral peaks and the appearance of new, very strong absorption peaks at 319, 395, and 715 cm^{-1}, all of which originate from the strong electron-phonon coupling between the SWCNT excitons and the S-S vibrations[129]. These findings provide new points to explain previously reported Raman signal abnormal phenomena for other filled CNTs heterostructures.

As a fingerprint characterization, Raman spectra are a simple and effective method to study the electronic structure of filled carbon-nanotube heterostructures. However, the disadvantages of Raman characterization are also obvious. For example, other morphological characterization methods are required for carbon nanotube positioning during large-area characterization. The characterization efficiency is very low when point-by-point scanning is used[126].

X-ray absorption spectrum (XAS)

X-ray absorption spectrum (XAS) refers to the measurement of the attenuation of X-rays as they pass through a material at varying energies. It provides information about the electronic structure and chemical composition of the material, including the types of atoms present, their oxidation states, and their coordination environments. This is achieved by examining the energy-dependent changes in the absorption of X-rays due to different core-level transitions in the atoms of the material[130]. XAS has several advantages and limitations. One of the main advantages is its ability to provide information on the local structure of a material at the atomic level, including the valence state and coordination geometry of the absorbing atom. XAS is also a non-destructive technique, allowing for the repeated analysis of a sample without altering its properties. However, XAS has some limitations, such as providing information only on the absorbing atom and not the surrounding environment. The XAS spectrum of SWCNTs filled with FeX_2[115], NiX_2[124], ZnX_2[104], CdX_2[116], AgX[102], CuX (X = Cl, Br, I)[103], $HgCl_2$[131] and other substances has been documented in the literatures.

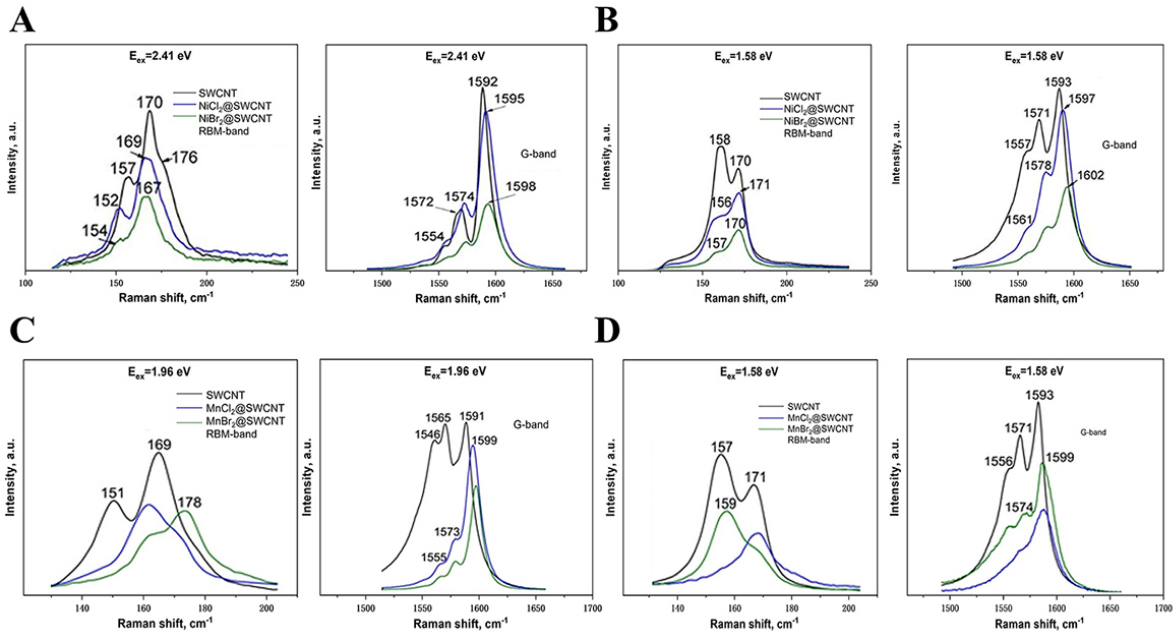

Figure 7. Raman characterization of carbon-nanotube nanopeapods: (A) Raman of MnX_2@SWCNT heterostructures at 1.96 eV laser energy (Reproduced with permission[123]. Copyright 2012, IOP Science). (B) Raman of MnX_2@SWCNTs heterostructures at 1.58 eV laser energy (Reproduced with permission[123]. Copyright 2012, IOP Science). (C) Raman of SWCNTs and NiX_2@SWCNTs at 2.41 eV laser energy (Reproduced with permission[124]. Copyright 2012, Wiley). (D) Raman of SWCNTs and NiX_2@SWCNTs at 1.58 eV laser energy (Reproduced with permission[124]. Copyright 2012, Wiley).

XAS spectra of NiX_2@SWCNTs (X = Cl, Br) heterostructures measured by Kharlamova *et al.* are shown in Figure 8A[124]. Partial information on nickel halide nanotubes can be obtained from the absorption peaks of C 1s. C 1s can be simply understood as the minimum energy required to excite an electron in a 1s orbital. An additional spectral feature A* appears below the p formant A. This property can be attributed to the interaction between the wall and the filling material. Compared with the spectra of AgX@SWCNTs and the original nanotubes [Figure 8B], SWCNTs interact with the AgX crystal of the plugged layer[102]. This additional spectrum characteristic can be attributed to the energy level that is reduced by electron transition to the reduction of the transfer of the plug-in charge.

FUNCTIONAL APPLICATIONS OF FILLED CARBON-NANOTUBE HETEROSTRUCTURES

Carbon nanotubes have excellent conductivity[132], optical[133], and thermal properties[5], mechanical properties[4], and flexibility[134], which can be applied to them in nano-electronics[2], photovoltaic[135], thermoelectric power generation[136], energy storage[137], catalytic[138], and other important areas. SWCNTs can be a metal or semiconductor, depending on their atomic structure[139]. The method of filling can not only control its electronic structure[12] but also retain the above many excellent properties, which greatly accelerates the industrialization application of carbon nanotubes.

Nanoelectronics

Charge transfer between the filled materials and CNT is common, which alters the electrical transport properties in a CNT. Li *et al.* prepared field-effect transistors (FET) with C_{60} and C_{70}@SWCNT peapods as channel materials and measured the transfer characteristics at room temperature [Figure 9A][26]. The I_{DS}-V_g curves of the C_{60} and C_{70} peapods FET show P-type hole-dominate transport characteristics, which are similar to those of pristine SWCNTs. When C_{60} is replaced with azafullerene ($C_{59}N$ and $C_{69}N$), the FETs exhibit typical N-type electron-dominate transport characteristics [Figure 9B][26]. Furthermore, a

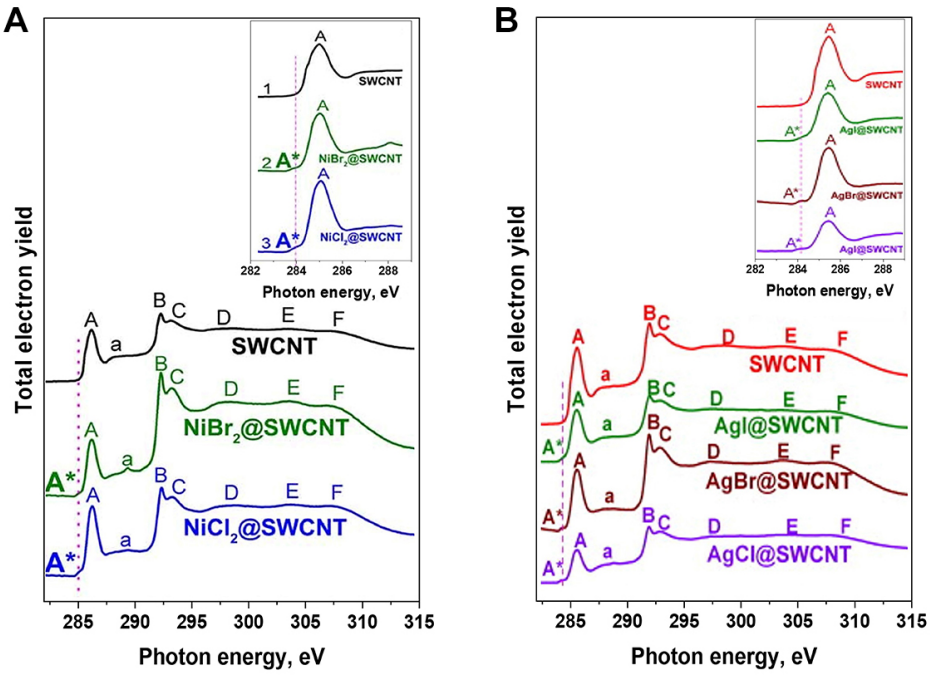

Figure 8. XAS characterization of carbon-nanotube nanopeapods: (A) XAS of SWCNTs and NiX_2@SWCNTs (X = Cl, Br) (Reproduced with permission[124]. Copyright 2012, Wiley). (B) XAS of SWCNTs and AgX@SWCNTs (X = Cl, Br, I) (Reproduced with permission[102]. Copyright 2010, Elsevier).

photoswitching behavior was also observed in $C_{59}N$ peapods FET devices, indicating the charge transfer from azafullerene to SWCNT [Figure 9C][140]. Shimada *et al.* investigated the transport characteristics of M@C_{82} (M = Gd, Dy) metallofullerenes nanopeapods FETs with ambipolar behavior. However, in the case of C_{90}-peapods, all devices exhibited metallic properties [Figure 9D][63].

Yang *et al.* further studied the temperature-dependent charge transport characteristics of Dy@C_{82} peapods FET. A transition from p-type to n-type conduction has been observed as the temperature decreases from room temperature to 265 K, indicating that charge transfers from the Dy@C_{82} to the conductance band of carbon nanotubes at low temperatures [Figure 9E][23]. At a temperature lower than 215 K, metallic behavior occurred, suggesting that additional electrons are continuously injected into the conductance band, shifting the Fermi level into the conduction band. Under 75 K, the device became a single-electron transistor with irregular coulomb blockade oscillation, meaning that the inside Dy@C_{82} splits the tube into discrete quantum dots. The transport properties of other fullerene nanopeapods FET are also investigated [Figure 9F].

It is also possible to produce p-n junctions within individual CNTs by partially filling the acceptor or donor. The examples were demonstrated in the heterostructures of partially filled CsI, CsC_{60}[25], and Fe[141] nanoparticles inside the SWCNTs where ultimate heterostructures of electron donor and acceptor were realized within the cavity of a SWCNT, yielding the air-stable rectifying performance.

Additional means can be used to tune the properties of the heterostructure-based electronic device if the target filler substance has a unique property, such as a spin-crossover (SCO) molecule[96] or magnetic cluster[14]. Giménez-López Mdel *et al.* encapsulated Mn_{12}Ac, a single-molecule magnet (SMM), into MWCNTs, resulting in a new type of heterostructure that combines the magnetic properties of the SMM

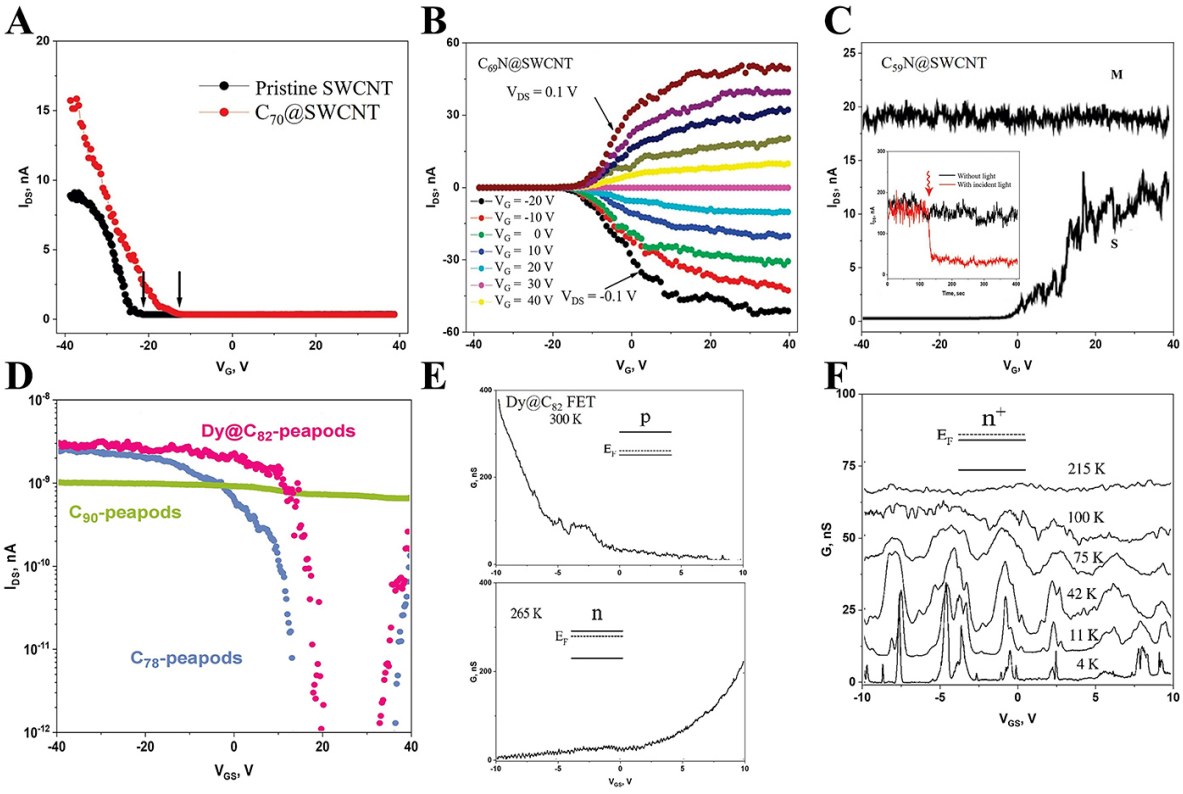

Figure 9. Electrical characterization of fullerene-peapods FETs: (A) Transfer curves for a pristine (unfilled) SWCNT FET and a C_{70} nanopeapods FET device (Reproduced with permission[26]. Copyright 2010, American Chemical Society). (B) Transfer curves measured for $C_{69}N$ nanopeapods FET (Reproduced with permission[26]. Copyright 2010, American Chemical Society). (C) I_{DS}-V_G characteristics measured at room temperature for an n-type semiconducting $C_{59}N$@SWCNT and a metallic $C_{59}N$@SWCNT without light (V_{DS} = 0.1 V). The inset shows the I_{DS} characteristic of the semiconducting $C_{59}N$@SWCNT, which is measured as a function of time without and with incident light (400 nm wavelength) (Reproduced with permission[140]. Copyright 2009, American Chemical Society). (D) Transfer characteristics of C_{78}, C_{90}, and Dy@C_{82}-peapods (V_{DS} = 20 mV, T = 23 K) (Reproduced with permission[63]. Copyright 2003, Elsevier). (E) V_G dependence of conductance measured at various temperatures (V_{DS} = 4) (Reproduced with permission[23]. Copyright 2001, AIP Publishing). (F) Conductance of Dy@C_{82}-peapods at temperatures from 4 to 215 K. The insets in (E) and (F) are band diagrams (Reproduced with permission[23]. Copyright 2001, AIP Publishing).

with the functional properties of the CNT [Figure 10][14]. At low temperatures, due to the molecule orientation of the SMM molecule arrangement inside the CNTs, the electrical resistance of the host CNTs exhibited anisotropic behavior. Villalva *et al.* synthesized the Fe-based SCO molecules filled SWCNTs heterostructures (Fe-SCO@SWCNT). The electronic transport measurements indicated that the SCO switch of the molecules triggers large conductance bistability via the SWCNT[96].

In the above, various nanoelectronic devices suggested that the filled CNT is an effective method for tuning and extending the function of pristine SWCNT.

Energy

Lithium-ion battery

Filling CNTs with suitable materials can increase their practical capacity, and their electrochemical properties are very suitable for battery preparation. Yu *et al.* tested the battery performance of FeS@CNTs [Figure 11A][54]. The battery was stable over multiple cycles, with higher cycle stability per cycle than graphite and FeS batteries. Another paper[142] demonstrated that even after one thousand cycles at a highly charged current of 2,000 mA g^{-1}, the FeS_2@CNTs battery could achieve a specific capacity of 525 mAh g^{-1}.

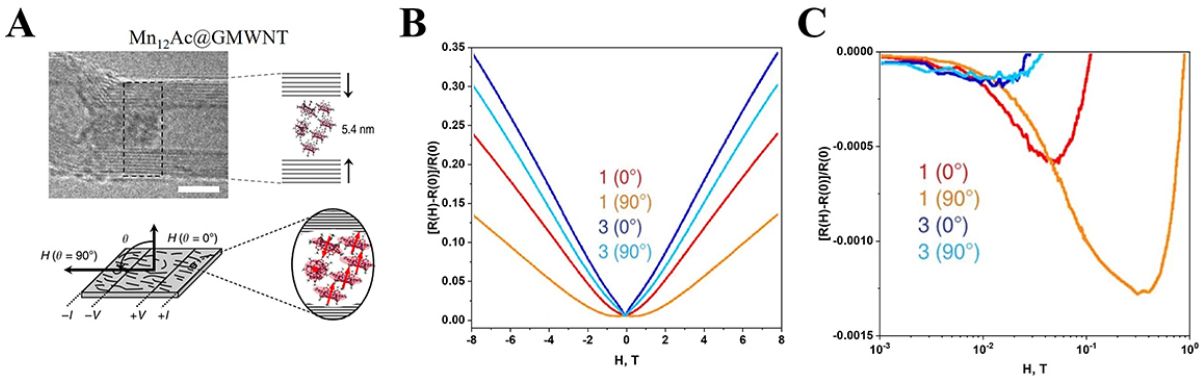

Figure 10. Effect of magnetic molecular filling on the resistance of CNTs (Reproduced with permission[14]. Copyright 2011, Springer Nature): (A) TEM of MWCNT filled with $Mn_{12}Ac$, scale bar is 5 nm, and schematic of magnetoresistance measurement apparatus and $Mn_{12}Ac$ molecules filled in CNTs. (B) Magnetoresistance of $Mn_{12}Ac$@MWCNT (1) and the control sample of pristine MWCNT (3) at 2 K in the presence of a magnetic field (H) either perpendicular (θ = 0°) or parallel (θ = 90°) to the conducting layers. (C) Low field region of the magnetoresistance measurements.

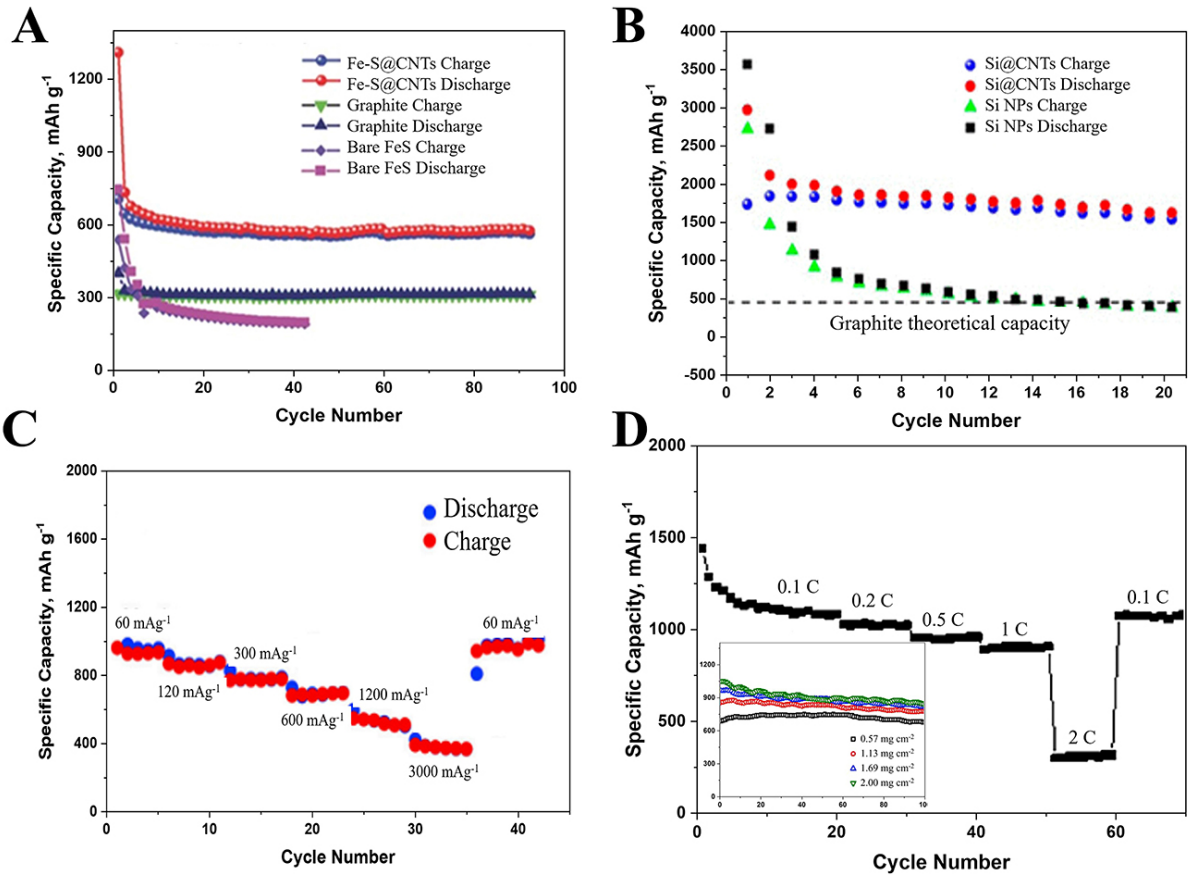

Figure 11. Properties of CNTs-filled lithium batteries: (A) Comparison of cyclic properties of three materials (Reproduced with permission[54]. Copyright 2016, Wiley). (B) Comparison of cycling properties of Si nanoparticles and Si nanoparticles@CNTs (Reproduced with permission[143]. Copyright 2015, American Chemical Society). (C) Cyclic performance of Fe_2O_3@CNTs at different current densities (Reproduced with permission[144]. Copyright 2017, American Chemical Society). (D) Rate performance of Li_2S_6@CNT thin film electrodes in the range of 0.1-2 C current density. Inset: the relationship between cycling performance and the weight of the CNTs film (Reproduced with permission[146]. Copyright 2017, Elsevier).

The reversible capacity of the Si nanoparticle @CNTs cell after 20 cycles is 1,475 mAh g^{-1} [Figure 11B], which is approximately four times that of graphite[143].

The cyclic performance of the cell prepared with Fe_2O_3@CNTs is shown in Figure 11C[144]. When the current density is 1,200 mA g^{-1}, approximately 40% of the capacity remains, and when the current rate is decreased to 60 mA g^{-1}, approximately 1,000 mA g^{-1} reversible capacity remains. Fe_3O_4-filled MWCNTs have also been studied as anode materials[145]. The specific capacity reached 220 mAh g^{-1} after 350 cycles, roughly twice that of unfilled CNTs at a current density of 2,000 mA g^{-1}. Fe_3O_4 NPs trapped within CNTs enhance the electrochemical behavior of Li-ion batteries while also preventing structural degradation.

Li-S composite system as the electrode material of high-performance batteries has been widely concerned. Kim *et al.* prepared lithium batteries using Li_2S_6@CNT conductive thin films as electrode materials and tested their performance [Figure 11D][146]. As the current density reduces from 0.1 C to 2 C, the discharge capacity decreases gradually. At the end of the cycle, when the current density returns to the initial level, the specific capacity is 1,081 mAh g^{-1} (initially 1,090 mAh g^{-1}), suggesting that the electrode has excellent stability. The illustration shows the relationship between cycle performance and film quality. This may be due to the increase in weight of CNT film, which leads to an increase in active adsorption sites in its interior, which is very favorable for the improvement of battery performance. Furthermore, Fu *et al.* investigated the chemical properties of sulfur in two types of SWCNTs with distinct diameters, produced by an electric arc (EA-SWCNTs, average diameter 1.55 nm) or high-pressure carbon monoxide (HiPco-SWCNTs, average diameter 1.0 nm), and demonstrated the electrochemical reaction activity of sulfur with lithium inside SWCNTs of different diameters[78]. Specifically, relatively larger diameter EA-SWCNTs can accommodate dissolved Li^+ ions, similar to Li-S reactions in solution. In contrast, Li^+ ions are blocked from entering the tube cavity in smaller diameter HiPco-SWCNTs. Therefore, the Li-S reaction in HiPco-SWCNTs is significantly different from when S is not encapsulated and can be attributed to interactions with π electrons passing through the carbon walls. This finding provides a new mechanism for improving the performance of lithium-ion batteries by filling CNTs.

It should be noted that the function of carbon nanotubes is more like a modifier: their participation mainly serves to modify the storage of lithium, thereby enhancing the capacity of lithium-ion batteries. However, pure carbon nanotubes are not very effective as electrode materials[147]. When filling carbon nanotubes, the mass ratio with the active material is generally 1:5, in the milligram range. If pure carbon nanotubes are used as electrode materials, they exhibit high specific capacity in the first lithium-ion insertion step but cannot be fully released in the subsequent lithium-ion extraction process[148]. This means that a large portion of the lithium ions is irreversibly consumed, leading to a decrease in the Coulombic efficiency of the battery.

The cycling rate is reflected in the electrochemical stability of the material during battery charging and discharging cycles, as well as the efficiency of ion insertion and extraction processes and the degree of material damage. CNTs can significantly improve the cycling rate performance of lithium-ion batteries, mainly due to their conductivity, their special hollow tubular structure, and cross-linked network structure, which enhance the efficiency of electron conduction in electrode materials and improve ion transport in CNTs. Firstly, CNTs provide a fast ion transport path, thereby improving the electrochemical reaction of lithium storage. Secondly, the confinement effect of CNTs allows the encapsulated active electrode material to be in close contact with the carbon tubes, shortening the distance of electron and Li^+ ion transport, which is superior to loose materials. Finally, the cross-linked conductive CNT network disperses the stress concentration phenomenon of materials, enhancing the structural strength of powder materials. The carbon nanotubes also have enough space to release induced stress expansion during the charge/discharge process,

maintaining their structural stability, so the performance of filled carbon nanotubes is significantly better than that of traditional anode materials.

Although filled carbon nanotubes show superior electrochemical performance, their performance slightly decreases during cycling due to the instability of the electrode structure, including active and non-active materials such as carbon nanotubes filled with active particles and binders. The significant expansion of carbon nanotubes during lithiation can cause cracking, deformation, and partial peeling of the electrode components during cycling, leading to the deterioration of cycling performance. To address these issues, it is important to identify the optimal filling rate for different active materials to ensure the structural stability of the expanded electrode. The use of multi-walled carbon nanotubes can further limit the range of volume expansion. Designing the battery structure based on specific materials can also improve its overall electrochemical performance.

The thermoelectric power generation

A major concern has been the potential effect of molecules encapsulated in CNTs on the thermal properties of heterostructure systems. Kodama *et al.* developed a micro-nano processing method for determining the effect of filling on thermal conductivity (κ) and thermoelectric potential (S), as shown in Figure 12[149]. The results show that the filled CNTs reduce thermal conductivity by 35%-55% and increase thermoelectric potential by about 40% compared to pristine CNTs at room temperature. Temperature-dependent measurements from 40 to 320 K show that the peak of thermal conductivity changes as temperature decreases.

Fukumaru *et al.* investigated the thermoelectric characteristics of $CoCp_2$@SWCNT heterostructures[150]. Compared with original SWCNTs, the electrical conductivity of the heterostructures was significantly improved by an order of magnitude. The negative Seebeck coefficient of -41.8 mV K^{-1} at 320 K indicates that encapsulation of cobaltocene can convert the p-type pristine semiconducting SWCNT into an n-type. Furthermore, the heterostructure has a high power factor and a low thermal conductivity (0.15 W m^{-1} K^{-1}). Such a heterogeneous structure of conductivity, power factor, and thermal conductivity is very suitable for the thermoelectric generation and is an attractive choice for the next generation of thermoelectric appliances.

Catalyst

CNTs with a large internal surface area are very stable and good catalyst carriers. Their main function is to immobilize and load nanoparticles and to provide an ideal local environment for certain chemical reactions. Aygün *et al.* investigated the catalytic performance of Ru@SWCNTs *vs.* Ru coated on the surface of SWCNTs[151]. It has been demonstrated that the reason for improving the catalytic efficiency is not only the stabilization of the catalytic particles but also the increase in the local concentration of the reactant precursor, which is critical to the catalytic effect. Chamberlain *et al.* decompose synthetic catalytic nanoparticles in SWCNTs[152]. The size and morphology of the nanoclusters were controlled by the diameter of SWCNTs, and efficient nanoparticle-filled SWCNTs provided a suitable environment for hydrogenation. SWCNTs with different diameters can compare nanometers of different sizes, which is critical for catalytic activity. The life of nanoparticles packed steadily into carbon nanotubes would be greatly extended.

Che *et al.* prepared highly aligned and monodisperse graphite-carbon nanoarrays using alumina films as templates and filled carbon nanotubes with nanoparticles (Ru and Pt/Ru)[153]. Supported catalysts are used in electrocatalytic oxygen reduction and methanol oxidation of hydrocarbons. The catalytic activity was significantly enhanced when CO and H_2O were converted to ethanol using Ru@CNTs.

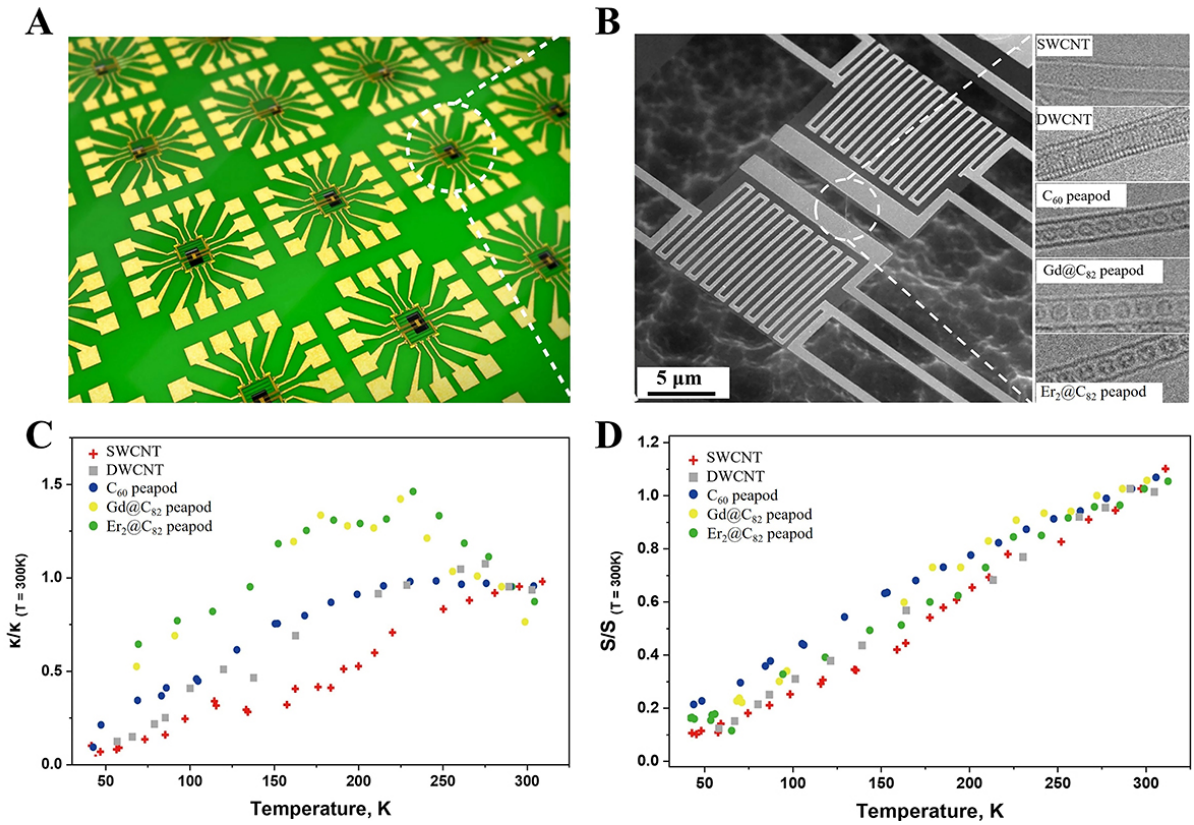

Figure 12. Properties of CNTs-filled in a thermoelectric generation (Reproduced with permission[149]. Copyright 2017, Springer Nature): (A) Schematic diagram of measuring equipment. (B) TEM photos of measuring device details. (C and D) The relationship between κ and S of CNTs and temperature after filling C_{60}, $Gd@C_{82}$, and $Er_2@C_{82}$.

Sensor

The 1D electronic properties and large adsorption area of SWCNTs can also be applied to gas sensors[154]. The ideal sensor should be highly selective[155], highly sensitive[156], completely recyclable[157], durable[158], and low in cost[159]. Although pure SWCNTs show neither specificity for gases nor are they gas-sensitive materials[160], the selection of suitable materials for filling can confer selectivity and sensitivity to X@SWCNTs heterostructures. Chimowa *et al.* used DWCNTs filled with ZnI_2 as a formaldehyde sensor[24]. The study demonstrates that it is possible to enhance the sensitivity and selectivity of the sensor by filling DWCNT. The performance of this filling is better than the surface function of nanotubes. Quang *et al.* reported the effects of ammonia adsorption at various temperatures on the electrical performance of SWCNT[161]. When the concentration of NH_3 was as low as 5 ppm, they were still able to detect the sensor's reaction to NH_3 and showed a good linear relationship. There is no obvious sign of saturation in the linear response area of the ~40 ppm concentration. Under a higher concentration, the reaction is sub-linear, but the reaction continues to increase as the concentration level increases. Nguyen *et al.* tested NH_3 sensors based on SWCNT devices under constant current conditions. The sensor's recovery and exposure time were determined by controlling the NH_3 concentration at 5 ppm[162]. After 10 min of exposure to NH_3, the electrical resistance increased by 8%. Qi *et al.* prepare a large-scale array of low-noise electronic CNT sensors for detecting gas molecules[163]. The functionalization of polymers makes SWCNTs resistant with high sensitivity and selectivity. Polyethylene amine coatings enable nanotube devices to detect nitric oxide at levels as low as 1 ppb (one billionth). Ramachandran *et al.* filled multi-wall carbon nanotubes with Ni-Co alloy nanowires for non-enzyme electrochemical sensor probes that reliably detect glucose[164]. The

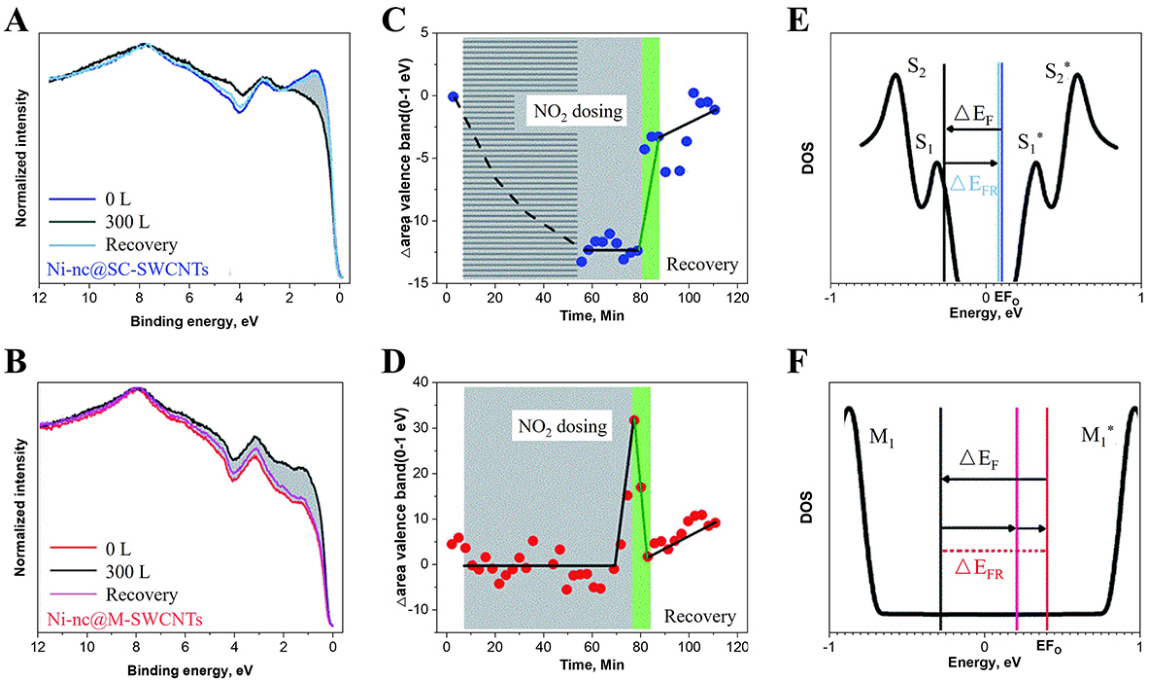

Figure 13. Properties of CNTs-filled sensors for NO_2 gas (Reproduced with permission[166]. Copyright 2020, The Royal Society of Chemistry): (A and B) Photoemission spectra of Ni@sCNTs and Ni@mCNTs, respectively. (C and D) Recovery time of Ni@sCNTs and Ni@mCNTs, respectively. (E and F) Fermi level density offset plot for Ni@sCNTs and Ni@mCNTs, respectively.

outstanding electrochemical properties of the sensor are attributed to the synergy of the Ni-Co@MWCNT heterostructure. Chimowa *et al.* proposed vanadium oxide-filled MWCNTs for methane gas sensors[165]. They observed that the response time for methane gas detection decreased from 140 s (not filled) to 17 s (after filling), and the recovery time decreased from 235 s to 120 s. As a result of the metal oxide filling, the response sensitivity of the CNT was increased from 0.5% to 1.5%.

Fedi *et al.* demonstrated the feasibility of acetone nickel molecules filled SWCNTs to detect the feasibility of nitric oxide [Figure 13][166]. Figure 13A and B depict the optoelectronic transmission spectrum of the semiconductor and metal SWCNTs of Ni clusters before and after exposure to NO_2. The shaded areas in Figure 13C and D represent a 30-minute recovery time after 80 min of continuous exposure at a total NO_2 flow rate of 300 L. After 3 min, the light green stripes indicate that the recovery is nearly complete. Figure 13E and F represent the Ni cluster's Fermi level density and the Fermi level state density shift of Ni cluster metal SWCNTs. The interaction between nanotubes and sensor targets can be finely tuned by filling SWCNTs, allowing for gas adsorption and adsorption at room temperature.

CONCLUSIONS

Because of their unique properties, CNTs are a promising material in a variety of applications involving electronics, energy, and catalysis. In the last decade years, it has been experimentally demonstrated that replacing carbon atoms with other atoms, adding functional groups to the outer nanotube surface non-covalently or covalently, and filling the CNT channels are all effective ways to change the CNTs' electronic structure. This has enriched the variety of CNTs' applications and electronic properties. Filling the CNT channels is the most promising way of these to modify the nanotube characteristics because various functional materials can be encapsulated into the CNT inner channel to generate heterostructures without damaging the carbon wall structure.

In the present manuscript, we concentrated on an overview of the preparation, morphological and electronic structure characterization, and applications of filled CNTs heterostructures. With the aid of the advanced HR-TEM and AC-TEM techniques, the structures of the internal substances filling in the heterostructures are thoroughly examined *in situ*. Due to the spatial confinement effect of CNT, for some substances, the structures inside the CNT are significantly different from the bulk state and sensitive to the diameter of the CNT, which can be manipulated to design its electronic behavior. Various unstable nanomaterials have been achieved through nano chemical reactions inside the nanotubes, suggesting that the confined hollow nano space of CNTs serves as a platform for novel nanomaterials. Furthermore, spectroscopic techniques like OAS, Raman, and XAS provide researchers with simple approaches to investigate the modified electronic properties of nanotubes that occur as a result of the encapsulation of various compounds inside their channels. For example, both P and N doping of the CNT were observed when the electron donor and electron acceptor were filled. Therefore, the established methods and knowledge for modifying the electronic properties of CNTs provide the fundamentals for functioning CNTs devices.

Although various filled CNTs heterostructures have been synthesized, many challenges remain for further large-scale applications. First of all, many external factors affect the filling process, leading to low reproducibility of internal filling quality and filling yield. Therefore, it is necessary to explore and summarize more experienced filling mechanisms to guide the synthesis of high-quality samples. The yield of CNT filling may vary due to various factors, such as the size of CNTs, the properties of filling materials, the filling method, and the conditions of filling. In some cases, the yield may be high, even close to 100%, while in other cases, the yield may be relatively low or even unable to fill. Regarding the practical aspects of CNT filling, it is important to consider the expected applications and required characteristics of the filled CNTs. For example, if the filled CNTs are intended to be used as catalyst supports, the filling material should be selected based on its catalytic activity and stability, and the filling process should be optimized to ensure uniform distribution of the filling material throughout the CNTs. The filling method also has practical significance. For example, if a solvent-based filling method is used, it may be difficult to completely remove the solvent from the filled CNTs, which can affect the final performance of the material. Second, the nature of heterostructures has not been investigated in depth. Based on obtaining high-quality heterostructure samples, understanding the structural, electrical, and spectral properties of the sample from the perspective of a single tube is the next essential step in further applications. Third, it is difficult to separate high-purity semiconducting filled CNTs heterostructures for field-effect transistor applications. When the SWCNT is filled with substance, the weight and surface charge distribution of the CNT are both altered, resulting in mature separation conditions that are no longer applicable. Finally, in scenarios where filled carbon nanotubes are used in vacuum or liquid media, there is a potential for the filling material to diffuse out, reducing the stability of the structure. One potential method to minimize diffusion is to functionalize the CNT walls with appropriate chemical groups, which can help immobilize the guest material inside the CNT. Another approach is to use encapsulation techniques, such as coating the CNT with protective layers or combining the filled CNT with larger composite materials.

In conclusion, despite many challenges, the filled CNTs heterostructures would provide abundant opportunities for future interdisciplinary fundamental research and emerging applications in nanoelectronic devices, energy, storage, catalysis, and other fields.

DECLARATIONS

Authors' contributions

Conducted the literature review and drafted the original version: Teng Y, Li J

Revised the manuscript: Teng Y, Li J, Yao J, Kang L, Li Q
Conceived and supervised the project: Kang L, Li Q

Availability of data and materials
Not applicable.

Financial support and sponsorship
The authors are grateful for the technical support for Nano-X from Suzhou Institute of Nano-Tech and Nano-Bionics, Chinese Academy of Sciences (SINANO). This work was supported by the Jiangsu Province Youth Fund (BK20220289), the China Postdoctoral Science Foundation (Grant No.2022M720104), and Jiangsu Funding Program for Excellent Postdoctoral Talent.

Conflicts of interest
All authors declared that there are no conflicts of interest.

Ethical approval and consent to participate
Not applicable.

Consent for publication
Not applicable.

REFERENCES
1. Iijima S. Helical microtubules of graphitic carbon. *Nature* 1991;354:56-8. DOI
2. Peng L, Zhang Z, Qiu C. Carbon nanotube digital electronics. *Nat Electron* 2019;2:499-505. DOI
3. Saito R, Nugraha ART, Hasdeo EH, Hung NT, Izumida W. Electronic and optical properties of single wall carbon nanotubes. *Top Curr Chem* 2017;375:7. DOI PubMed
4. Yi C, Chen X, Gou F, et al. Direct measurements of the mechanical strength of carbon nanotube - aluminum interfaces. *Carbon* 2017;125:93-102. DOI
5. Zhou K, Xu N, Xie G. Thermal conductivity of carbon nanotube superlattices: comparative study with defective carbon nanotubes. *Chin Phys B* 2018;27:026501. DOI
6. Wan H, Cao Y, Lo LW, Zhao J, Sepúlveda N, Wang C. Flexible carbon nanotube synaptic transistor for neurological electronic skin applications. *ACS Nano* 2020;14:10402-12. DOI PubMed
7. Zang M. Band theory of single-walled carbon nanotubes. *IEEE Trans Nanotechnol* 2005;4:452-9. DOI
8. Desai SB, Madhvapathy SR, Sachid AB, et al. MoS_2 transistors with 1-nanometer gate lengths. *Science* 2016;354:99-102. DOI PubMed
9. Srimani T, Ding J, Yu A, et al. Comprehensive study on high purity semiconducting carbon nanotube extraction. *Adv Electron Mater* 2022;8:2101377. DOI
10. Dekker C. How we made the carbon nanotube transistor. *Nat Electron* 2018;1:518-518. DOI
11. Clément P, Xu X, Stoppiello CT, et al. Direct synthesis of multiplexed metal-nanowire-based devices by using carbon nanotubes as vector templates. *Angew Chem Int Ed* 2019;58:9928-32. DOI PubMed
12. Zhao C, Zhou X, Xie S, et al. DFT study of electronic structure and properties of N, Si and Pd-doped carbon nanotubes. *Ceram Int* 2018;44:21027-33. DOI
13. Ajayan PM, Iijima S. Capillarity-induced filling of carbon nanotubes. *Nature* 1993;361:333-4. DOI
14. Giménez-López Mdel C, Moro F, La Torre A, et al. Encapsulation of single-molecule magnets in carbon nanotubes. *Nat Commun* 2011;2:407. DOI PubMed
15. Haft M, Grönke M, Gellesch M, et al. Tailored nanoparticles and wires of Sn, Ge and Pb inside carbon nanotubes. *Carbon* 2016;101:352-60. DOI
16. Talyzin AV, Anoshkin IV, Krasheninnikov AV, et al. Synthesis of graphene nanoribbons encapsulated in single-walled carbon nanotubes. *Nano Lett* 2011;11:4352-6. DOI PubMed
17. Kharlamova MV, Kramberger C, Saito T, Pichler T. Diameter and metal-dependent growth properties of inner tubes inside

metallocene-filled single-walled carbon nanotubes. *Fuller Nanotub Carbon Nanostruct* 2020;28:20-6. DOI

18. Vasylenko A, Marks S, Wynn JM, et al. Electronic structure control of sub-nanometer 1D SnTe via Nanostructuring within single-walled carbon nanotubes. *ACS Nano* 2018;12:6023-31. DOI PubMed
19. Koizumi R, Hart AH, Brunetto G, et al. Mechano-chemical stabilization of three-dimensional carbon nanotube aggregates. *Carbon* 2016;110:27-33. DOI
20. Pan X, Bao X. The effects of confinement inside carbon nanotubes on catalysis. *ACC Chem Res* 2011;44:553-62. DOI PubMed
21. Nieto-Ortega B, Villalva J, Vera-Hidalgo M, Ruiz-González L, Burzurí E, Pérez EM. Band-gap opening in metallic single-walled carbon nanotubes by encapsulation of an organic salt. *Angew Chem Int Ed* 2017;56:12240-4. DOI PubMed
22. Ivanov VG, Kalashnyk N, Sloan J, Faulques E. Vibrational dynamics of extreme 2 × 2 and 3 × 3 potassium iodide nanowires encapsulated in single-walled carbon nanotubes. *Phys Rev B* 2018;98:125429. DOI
23. Chiu PW, Gu G, Kim GT, et al. Temperature-induced change from p to n conduction in metallofullerene nanotube peapods. *Appl Phys Lett* 2001;79:3845-7. DOI
24. Chimowa G, Yang L, Lonchambon P, et al. Tailoring of double-walled carbon nanotubes for formaldehyde sensing through encapsulation of selected materials. *Phys Status Solidi A* 2019;216:1900279. DOI
25. Kato T, Hatakeyama R, Shishido J, Oohara W, Tohji K. P-N junction with donor and acceptor encapsulated single-walled carbon nanotubes. *Appl Phys Lett* 2009;95:083109. DOI
26. Li Y, Kaneko T, Miyanaga S, Hatakeyama R. Synthesis and property characterization of c(69)n azafullerene encapsulated single-walled carbon nanotubes. *ACS Nano* 2010;4:3522-6. DOI PubMed
27. Poudel YR, Li W. Synthesis, properties, and applications of carbon nanotubes filled with foreign materials: a review. *Mater Today Phys* 2018;7:7-34. DOI
28. Eliseev AA, Kharlamova MV, Chernysheva MV, et al. Preparation and properties of single-walled nanotubes filled with inorganic compounds. *Russ Chem Rev* 2009;78:833-54. DOI
29. Yang Q, Hou P, Bai S, Wang M, Cheng H. Adsorption and capillarity of nitrogen in aggregated multi-walled carbon nanotubes. *Chem Phys Lett* 2001;345:18-24. DOI
30. Wilder JWG, Venema LC, Rinzler AG, Smalley RE, Dekker C. Electronic structure of atomically resolved carbon nanotubes. *Nature* 1998;391:59-62. DOI
31. Dujardin E, Ebbesen TW, Hiura H, Tanigaki K. Capillarity and wetting of carbon nanotubes. *Science* 1994;265:1850-2. DOI PubMed
32. Ruoff RS, Lorents DC, Chan B, Malhotra R, Subramoney S. Single crystal metals encapsulated in carbon nanoparticles. *Science* 1993;259:346-8. DOI PubMed
33. Guerret-piécourt C, Bouar YL, Lolseau A, Pascard H. Relation between metal electronic structure and morphology of metal compounds inside carbon nanotubes. *Nature* 1994;372:761-5. DOI
34. Hsu W, Li J, Terrones H, et al. Electrochemical production of low-melting metal nanowires. *Chem Phys Lett* 1999;301:159-66. DOI
35. Hirahara K, Suenaga K, Bandow S, et al. One-dimensional metallofullerene crystal generated inside single-walled carbon nanotubes. *Phys Rev Lett* 2000;85:5384-7. DOI PubMed
36. Tobias G, Shao L, Salzmann CG, Huh Y, Green ML. Purification and opening of carbon nanotubes using steam. *J Phys Chem B* 2006;110:22318-22. DOI PubMed
37. Ajayan PM, Ebbesen TW, Ichihashi T, Iijima S, Tanigaki K, Hiura H. Opening carbon nanotubes with oxygen and implications for filling. *Nature* 1993;362:522-5. DOI
38. Tsang SC, Chen YK, Harris PJF, Green MLH. A simple chemical method of opening and filling carbon nanotubes. *Nature* 1994;372:159-62. DOI
39. Hernadi K, Siska A, Thiên-nga L, Forró L, Kiricsi I. Reactivity of different kinds of carbon during oxidative purification of catalytically prepared carbon nanotubes. *Solid State Ion* 2001;141-142:203-9. DOI
40. Wiśniewski M, Terzyk AP, Hattori Y, Kaneko K, Okino F, Kruszka B. Hydrothermal opening of multiwall carbon nanotube with H_2O_2 solution. *Chem Phys Lett* 2009;482:316-9. DOI
41. Ribeiro H, Schnitzler MC, da Silva WM, Santos AP. Purification of carbon nanotubes produced by the electric arc-discharge method. *Surf Interfaces* 2021;26:101389. DOI
42. Egemen E, Nirmalakhandan N, Trevizo C. Predicting surface tension of liquid organic solvents. *Environ Sci Technol* 2000;34:2596-600. DOI
43. Eliseev A, Yashina L, Kharlamova M, Kiselev N. One-dimensional crystals inside single-walled carbon nanotubes: growth, structure and electronic properties. In: Electronic properties of carbon nanotubes. 2011. DOI
44. Sloan J, Kirkland AI, Hutchison JL, Green ML. Structural characterization of atomically regulated nanocrystals formed within single-walled carbon nanotubes using electron microscopy. *ACC Chem Res* 2002;35:1054-62. DOI PubMed
45. Wang D, Saleem MF, Javid M, et al. Formation of Sn filled CNTs nanocomposite: study of their magnetic, dielectric properties and enhanced microwave absorption performance at gigahertz frequencies. *Ceram Int* 2022;48:21961-71. DOI
46. Fujimori T, Morelos-Gómez A, Zhu Z, et al. Conducting linear chains of sulphur inside carbon nanotubes. *Nat Commun* 2013;4:2162. DOI
47. Belandria E, Millot M, Broto J, et al. Pressure dependence of Raman modes in double wall carbon nanotubes filled with 1D Tellurium. *Carbon* 2010;48:2566-72. DOI

48. Kitaura R, Nakanishi R, Saito T, Yoshikawa H, Awaga K, Shinohara H. High-yield synthesis of ultrathin metal nanowires in carbon nanotubes. *Angew Chem Int Ed* 2009;48:8298-302. DOI PubMed
49. Kharlamova MV. Comparative analysis of electronic properties of tin, gallium, and bismuth chalcogenide-filled single-walled carbon nanotubes. *J Mater Sci* 2014;49:8402-11. DOI
50. Stonemeyer S, Cain JD, Oh S, et al. Stabilization of $NbTe_3$, VTe_3 and $TiTe_3$ via nanotube encapsulation. *J Am Chem Soc* 2021;143:4563-8. DOI PubMed
51. Pham T, Oh S, Stetz P, et al. Torsional instability in the single-chain limit of a transition metal trichalcogenide. *Science* 2018;361:263-6. DOI PubMed
52. Kharlamova MV, Yashina LV, Lukashin AV. Comparison of modification of electronic properties of single-walled carbon nanotubes filled with metal halogenide, chalcogenide, and pure metal. *Appl Phys A* 2013;112:297-304. DOI
53. Kashtiban RJ, Patrick CE, Ramasse Q, Walton RI, Sloan J. Picoperovskites: the smallest conceivable isolated halide perovskite structures formed within carbon nanotubes. *Adv Mater* 2023;35:e2208575. DOI PubMed
54. Yu WJ, Liu C, Zhang L, et al. Synthesis and electrochemical lithium storage behavior of carbon nanotubes filled with iron sulfide nanoparticles. *Adv Sci* 2016;3:1600113. DOI PubMed PMC
55. Calatayud DG, Ge H, Kuganathan N, et al. Encapsulation of cadmium selenide nanocrystals in biocompatible nanotubes: DFT calculations, X-ray diffraction investigations, and confocal fluorescence imaging. *Chem Eur* 2018;7:144-58. DOI PubMed PMC
56. Norman LT, Biskupek J, Rance GA, Stoppiello CT, Kaiser U, Khlobystov AN. Synthesis of ultrathin rhenium disulfide nanoribbons using nano test tubes. *Nano Res* 2022;15:1282-7. DOI
57. Popple D, Dogan M, Hoang TV, et al. Charge-induced phase transition in encapsulated $HfTe_2$ nanoribbons. *Phys Rev Mater* 2023;7:L013001. DOI
58. Wang Z, Zhao K, Li H, et al. Ultra-narrow WS_2 nanoribbons encapsulated in carbon nanotubes. *J Mater Chem* 2011;21:171-80. DOI
59. Carter R, Suyetin M, Lister S, et al. Band gap expansion, shear inversion phase change behaviour and low-voltage induced crystal oscillation in low-dimensional tin selenide crystals. *Dalton Trans* 2014;43:7391-9. DOI PubMed
60. Wang Z, Li H, Liu Z, et al. Mixed low-dimensional nanomaterial: 2D ultranarrow MoS_2 inorganic nanoribbons encapsulated in quasi-1D carbon nanotubes. *J Am Chem Soc* 2010;132:13840-7. DOI PubMed
61. Koshino M, Niimi Y, Nakamura E, et al. Analysis of the reactivity and selectivity of fullerene dimerization reactions at the atomic level. *Nat Chem* 2010;2:117-24. DOI PubMed
62. Simon F, Kuzmany H, Rauf H, et al. Low temperature fullerene encapsulation in single wall carbon nanotubes: synthesis of N@C60@SWCNT. *Chem Phys Lett* 2004;383:362-7. DOI
63. Shimada T, Ohno Y, Okazaki T, et al. Transport properties of C78, C90 and Dy@C82 fullerenes-nanopeapods by field effect transistors. *Phys E Low Dimens Syst Nanostruct* 2004;21:1089-92. DOI
64. Luzzi DE, Smith BW, Russo R, et al. Encapsulation of metallofullerenes and metallocenes in carbon nanotubes. In AIP Conference Proceedings; 2001, pp. 622-6. DOI
65. Suenaga K, Hirahara K, Bandow S, et al. Core-level spectroscopy on the valence state of encaged metal in metallofullerene-peapods. In AIP Conference Proceedings; 2001, pp. 256-60. DOI
66. Suenaga K, Taniguchi R, Shimada T, Okazaki T, Shinohara H, Iijima S. Evidence for the intramolecular motion of Gd atoms in a $Gd_2@C_{92}$ nanopeapod. *Nano Lett* 2003;3:1395-8. DOI
67. Kuzmany H, Pfeiffer R, Simon F. The growth of nanophases in the clean room inside single-wall carbon nanotubes. *Synth Met* 2005;155:690-3. DOI
68. Zhong R, Tao J, Yang X, et al. Preparation of carbon nanotubes with high filling rate of copper nanoparticles. *Microporous Mesoporous Mater* 2022;344:112231. DOI
69. Lee J, Kim H, Kahng SJ, et al. Bandgap modulation of carbon nanotubes by encapsulated metallofullerenes. *Nature* 2002;415:1005-8. DOI PubMed
70. Botos A, Biskupek J, Chamberlain TW, et al. Carbon nanotubes as electrically active nanoreactors for multi-step inorganic synthesis: sequential transformations of molecules to nanoclusters and nanoclusters to nanoribbons. *J Am Chem Soc* 2016;138:8175-83. DOI PubMed
71. Béjar L, Mejía AA, Parra C, et al. Analysis of Raman spectroscopy and SEM of carbon nanotubes obtain by CVD. *Microsc Microanal* 2018;24:1092-3. DOI
72. Caccamo MT, Mavilia G, Magazù S. Thermal investigations on carbon nanotubes by spectroscopic techniques. *Appl Sci* 2020;10:8159. DOI
73. Banhart F. Irradiation of carbon nanotubes with a focused electron beam in the electron microscope. *J Mater Sci* 2006;41:4505-11. DOI
74. Oxley MP, Lupini AR, Pennycook SJ. Ultra-high resolution electron microscopy. *Rep Prog Phys* 2017;80:026101. DOI PubMed
75. Urban KW, Barthel J, Houben L, et al. Progress in atomic-resolution aberration corrected conventional transmission electron microscopy (CTEM). *Prog Mater Sci* 2023;133:101037. DOI
76. Guan L, Suenaga K, Shi Z, Gu Z, Iijima S. Polymorphic structures of iodine and their phase transition in confined nanospace. *Nano Lett* 2007;7:1532-5. DOI PubMed
77. Qin J, Liao P, Si M, et al. Raman response and transport properties of tellurium atomic chains encapsulated in nanotubes. *Nat Electron* 2020;3:141-7. DOI

78. Fu C, Oviedo MB, Zhu Y, et al. Confined lithium-sulfur reactions in narrow-diameter carbon nanotubes reveal enhanced electrochemical reactivity. *ACS Nano* 2018;12:9775-84. DOI PubMed
79. Corio P, Santos A, Santos P, et al. Characterization of single wall carbon nanotubes filled with silver and with chromium compounds. *Chem Phys Lett* 2004;383:475-80. DOI
80. Zhang J, Guo S, Wei J, et al. High-efficiency encapsulation of Pt nanoparticles into the channel of carbon nanotubes as an enhanced electrocatalyst for methanol oxidation. *Chemistry* 2013;19:16087-92. DOI PubMed
81. Kozhuharova R, Ritschel M, Elefant D, et al. Synthesis and characterization of aligned Fe-filled carbon nanotubes on silicon substrates. *J Mater Sci Mater Electron* 2003;14:789-91. DOI
82. Yao Y, Chen H, Lian C, et al. Fe, Co, Ni nanocrystals encapsulated in nitrogen-doped carbon nanotubes as Fenton-like catalysts for organic pollutant removal. *J Hazard Mater* 2016;314:129-39. DOI PubMed
83. Gao X, Zhang Y, Chen X, et al. Carbon nanotubes filled with metallic nanowires. *Carbon* 2004;42:47-52. DOI
84. Shi L, Rohringer P, Suenaga K, et al. Confined linear carbon chains as a route to bulk carbyne. *Nat Mater* 2016;15:634-9. DOI PubMed
85. Lenz K, Narkowicz R, Wagner K, et al. Magnetization dynamics of an individual single-crystalline Fe-filled carbon nanotube. *Small* 2019;15:e1904315. DOI PubMed
86. Aryee D, Seifu D. Shape anisotropy and hybridization enhanced magnetization in nanowires of Fe/MgO/Fe encapsulated in carbon nanotubes. *J Magn Magn Mater* 2017;429:161-5. DOI
87. Xu S, Li P, Lu Y. In situ atomic-scale analysis of Rayleigh instability in ultrathin gold nanowires. *Nano Res* 2018;11:625-32. DOI
88. Bingham JT, Proudian AP, Vyas S, Zimmerman JD. Understanding fragmentation of organic small molecules in atom probe tomography. *J Phys Chem Lett* 2021;12:10437-43. DOI PubMed
89. Jordan JW, Lowe GA, McSweeney RL, et al. Host-guest hybrid redox materials self-assembled from polyoxometalates and single-walled carbon nanotubes. *Adv Mater* 2019;31:e1904182. DOI PubMed
90. Smith BW, Monthioux M, Luzzi DE. Encapsulated C60 in carbon nanotubes. *Nature* 1998;396:323-4. DOI
91. Botos Á, Khlobystov AN, Botka B, et al. Investigation of fullerene encapsulation in carbon nanotubes using a complex approach based on vibrational spectroscopy. *Phys Status Solidi B* 2010;247:2743-5. DOI
92. Ashino M, Obergfell D, Haluska M, et al. Atomically resolved mechanical response of individual metallofullerene molecules confined inside carbon nanotubes. *Nat Nanotechnol* 2008;3:337-41. DOI PubMed
93. Khlobystov AN, Porfyrakis K, Kanai M, et al. Molecular motion of endohedral fullerenes in single-walled carbon nanotubes. *Angew Chem Int Ed* 2004;43:1386-9. DOI PubMed
94. Morgan DA, Sloan J, Green ML. Direct imaging of o-carborane molecules within single walled carbon nanotubes. *Chem Commun* 2002;20:2442-3. DOI PubMed
95. Khlobystov AN, Britz DA, Briggs GA. Molecules in carbon nanotubes. *ACC Chem Res* 2005;38:901-9. DOI PubMed
96. Villalva J, Develioglu A, Montenegro-Pohlhammer N, et al. Spin-state-dependent electrical conductivity in single-walled carbon nanotubes encapsulating spin-crossover molecules. *Nat Commun* 2021;12:1578. DOI PubMed PMC
97. Lee CH, Kang KT, Park KS, et al. The nano-memory devices of a single wall and peapod structural carbon nanotube field effect transistor. *Jpn J Appl Phys* 2003;42:5392-4. DOI
98. Friedrichs S, Sloan J, Green MLH, Meyer RR, Kirkland AI, Hutchison JL. Complete characterisation of a Sb_2O_3/(21,-8)SWNT inclusion composite. *Chem Commun* 2001;10:929-30. DOI
99. Brown G, Bailey SR, Sloan J, et al. Electron beam induced in situ clusterisation of 1D $ZrCl_4$ chains within single-walled carbon nanotubes. *Chem Commun* 2001;9:845-6. DOI
100. Eliseev AA, Chernysheva MV, Verbitskii NI, et al. Chemical reactions within single-walled carbon nanotube channels. *Chem Mater* 2009;21:5001-3. DOI
101. Nagata M, Shukla S, Nakanishi Y, et al. Isolation of single-wired transition-metal monochalcogenides by carbon nanotubes. *Nano Lett* 2019;19:4845-51. DOI PubMed
102. Eliseev A, Yashina L, Brzhezinskaya M, et al. Structure and electronic properties of AgX (X = Cl, Br, I)-intercalated single-walled carbon nanotubes. *Carbon* 2010;48:2708-21. DOI
103. Eliseev A, Yashina L, Verbitskiy N, et al. Interaction between single walled carbon nanotube and 1D crystal in CuX@SWCNT (X = Cl, Br, I) nanostructures. *Carbon* 2012;50:4021-39. DOI
104. Kharlamova MV, Yashina LV, Volykhov AA, et al. Acceptor doping of single-walled carbon nanotubes by encapsulation of zinc halogenides. *Eur Phys J B* 2012;85:34. DOI
105. Li L, Lin T, Doig J, et al. Crystal-encapsulation-induced band-structure change in single-walled carbon nanotubes: photoluminescence and Raman spectra. *Phys Rev B* 2006;74:245418. DOI
106. Stoppiello CT, Biskupek J, Li ZY, et al. A one-pot-one-reactant synthesis of platinum compounds at the nanoscale. *Nanoscale* 2017;9:14385-94. DOI PubMed
107. Cain JD, Oh S, Azizi A, et al. Ultranarrow TaS_2 nanoribbons. *Nano Lett* 2021;21:3211-7. DOI PubMed
108. Meyer S, Pham T, Oh S, et al. Metal-insulator transition in quasi-one-dimensional $HfTe_3$ in the few-chain limit. *Phys Rev B* 2019;100:4. DOI
109. Cabana L, Ballesteros B, Batista E, et al. Synthesis of PbI_2 single-layered inorganic nanotubes encapsulated within carbon nanotubes. *Adv Mater* 2014;26:2016-21. DOI PubMed

110. Wang L, Sofer Z, Bouša D, et al. Graphane nanostripes. *Angew Chem Int Ed* 2016;55:13965-9. DOI PubMed
111. Fu L, Shang C, Zhou S, Guo Y, Zhao J. Transition metal halide nanowires: a family of one-dimensional multifunctional building blocks. *Appl Phys Lett* 2022;120:023103. DOI
112. Kharlamova MV. Kinetics, electronic properties of filled carbon nanotubes investigated with spectroscopy for applications. *Nanomaterials* 2022;13:176. DOI PubMed PMC
113. Nonnenmacher M, Wickramasinghe H. Optical absorption spectroscopy by scanning force microscopy. *Ultramicroscopy* 1992;42-44:351-4. DOI
114. Kharlamova MV, Eliseev AA, Yashina LV, et al. Study of the electronic structure of single-walled carbon nanotubes filled with cobalt bromide. *JETP Lett* 2010;91:196-200. DOI
115. Kharlamova MV, Brzhezinskay MM, Vinogradov AS, et al. The formation and properties of one-dimensional $FeHal_2$ (Hal = Cl, Br, I) nanocrystals in channels of single-walled carbon nanotubes. *Nanotechnol Russ* 2009;4:634-46. DOI
116. Kharlamova MV, Yashina LV, Lukashin AV. Charge transfer in single-walled carbon nanotubes filled with cadmium halogenides. *J Mater Sci* 2013;48:8412-9. DOI
117. Kharlamova MV, Volykhov AA, Yashina LV, Egorov AV, Lukashin AV. Experimental and theoretical studies on the electronic properties of praseodymium chloride-filled single-walled carbon nanotubes. *J Mater Sci* 2015;50:5419-30. DOI
118. Kharlamova MV. Comparison of influence of incorporated 3d-, 4d- and 4f-metal chlorides on electronic properties of single-walled carbon nanotubes. *Appl Phys A* 2013;111:725-31. DOI
119. Kharlamova MV. Novel approach to tailoring the electronic properties of single-walled carbon nanotubes by the encapsulation of high-melting gallium selenide using a single-step process. *JETP Lett* 2013;98:272-7. DOI
120. Yashina LV, Eliseev AA, Kharlamova MV, et al. Growth and characterization of one-dimensional SnTe crystals within the single-walled carbon nanotube channels. *J Phys Chem C* 2011;115:3578-86. DOI
121. Si R, Fischer CF. Electron affinities of at and its homologous elements Cl, Br, and I. *Phys Rev A* 2018;98:052504. DOI
122. Jorio A, Saito R. Raman spectroscopy for carbon nanotube applications. *J Appl Phys* 2021;129:021102. DOI
123. Kharlamova MV, Eliseev AA, Yashina LV, Lukashin AV, Tretyakov YD. Synthesis of nanocomposites on basis of single-walled carbon nanotubes intercalated by manganese halogenides. *J Phys Conf Ser* 2012;345:012034. DOI
124. Kharlamova MV, Yashina LV, Eliseev AA, et al. Single-walled carbon nanotubes filled with nickel halogenides: atomic structure and doping effect. *Phys Status Solidi B* 2012;249:2328-32. DOI
125. Kharlamova MV, Kramberger C, Mittelberger A. Raman spectroscopy study of the doping effect of the encapsulated terbium halogenides on single-walled carbon nanotubes. *Appl Phys A* 2017;123:239. DOI
126. Kharlamova MV, Kramberger C, Pichler T. Semiconducting response in single-walled carbon nanotubes filled with cadmium chloride: semiconducting response in SWCNTs filled with $CdCl_2$. *Phys Status Solidi B* 2016;253:2433-9. DOI
127. Kharlamova MV, Sauer M, Saito T, et al. Doping of single-walled carbon nanotubes controlled via chemical transformation of encapsulated nickelocene. *Nanoscale* 2015;7:1383-91. DOI PubMed
128. Nascimento VV, Neves WQ, Alencar RS, et al. Origin of the giant enhanced raman scattering by sulfur chains encapsulated inside single-wall carbon nanotubes. *ACS Nano* 2021;15:8574-82. DOI PubMed
129. Li G, Fu C, Oviedo MB, et al. Giant Raman response to the encapsulation of sulfur in narrow diameter single-walled carbon nanotubes. *J Am Chem Soc* 2016;138:40-3. DOI PubMed
130. Mijit E, Trapananti A, Minicucci M, et al. Development of a high temperature diamond anvil cell for x ray absorption experiments under extreme conditions. *Radiat Phys Chem* 2020;175:108106. DOI
131. Fedoseeva YV, Orekhov AS, Chekhova GN, et al. Single-walled carbon nanotube reactor for redox transformation of mercury dichloride. *ACS Nano* 2017;11:8643-9. DOI PubMed
132. Gets AV, Krainov VP. Conductivity of single-walled carbon nanotubes. *J Exp Theor Phys* 2016;123:1084-9. DOI
133. Khosravi M, Badehian HA, Habibinejad M. Optical properties of double walled carbon nanotubes. *J Electron Spectros Relat Phenomena* 2021;248:147058. DOI
134. Shang Y, Hua C, Xu W, et al. Meter-long spiral carbon nanotube fibers show ultrauniformity and flexibility. *Nano Lett* 2016;16:1768-75. DOI PubMed
135. Chen C, Song C, Yang J, et al. Intramolecular p-i-n junction photovoltaic device based on selectively doped carbon nanotubes. *Nano Energy* 2017;32:280-6. DOI
136. Chiba T, Amma Y, Takashiri M. Heat source free water floating carbon nanotube thermoelectric generators. *Sci Rep* 2021;11:14707. DOI PubMed PMC
137. Wang JG, Liu H, Zhang X, Li X, Liu X, Kang F. Green synthesis of hierarchically porous carbon nanotubes as advanced materials for high-efficient energy storage. *Small* 2018;14:e1703950. DOI PubMed
138. Bychko IB, Abakumov AA, Lemesh NV, Strizhak PE. Catalytic activity of multiwalled carbon nanotubes in acetylene hydrogenation. *ChemCatChem* 2017;9:4470-4. DOI
139. Liu J, Lu J, Lin X, et al. The electronic properties of chiral carbon nanotubes. *Comput Mater Sci* 2017;129:290-4. DOI
140. Li Y, Kaneko T, Kong J, Hatakeyama R. Photoswitching in azafullerene encapsulated single-walled carbon nanotube FET devices. *J Am Chem Soc* 2009;131:3412-3. DOI PubMed
141. Li YF, Hatakeyama R, Shishido J, Kato T, Kaneko T. Air-stable p-n junction diodes based on single-walled carbon nanotubes encapsulating Fe nanoparticles. *Appl Phys Lett* 2007;90:173127. DOI

142. Xu L, Hu Y, Zhang H, Jiang H, Li C. Confined synthesis of FeS_2 nanoparticles encapsulated in carbon nanotube hybrids for ultrastable lithium-ion batteries. *ACS Sustain Chem Eng* 2016;4:4251-5. DOI
143. Yu WJ, Liu C, Hou PX, et al. Lithiation of silicon nanoparticles confined in carbon nanotubes. *ACS Nano* 2015;9:5063-71. DOI PubMed
144. Li S, Liu Y, Guo P, Wang C. Self-climbed amorphous carbon nanotubes filled with transition metal oxide nanoparticles for large rate and long lifespan anode materials in lithium ion batteries. *ACS Appl Mater Interfaces* 2017;9:26818-25. DOI PubMed
145. Liu Y, Wu N, Wang Z, Cao H, Liu J. Fe_3O_4 nanoparticles encapsulated in multi-walled carbon nanotubes possess superior lithium storage capability. *New J Chem* 2017;41:6241-50. DOI
146. Kim S, Song H, Jeong Y. Flexible catholyte@carbon nanotube film electrode for high-performance lithium sulfur battery. *Carbon* 2017;113:371-8. DOI
147. Landi BJ, Ganter MJ, Cress CD, Dileo RA, Raffaelle RP. Carbon nanotubes for lithium ion batteries. *Energy Environ Sci* 2009;2:638. DOI
148. Raccichini R, Varzi A, Passerini S, Scrosati B. The role of graphene for electrochemical energy storage. *Nat Mater* 2015;14:271-9. DOI PubMed
149. Kodama T, Ohnishi M, Park W, et al. Modulation of thermal and thermoelectric transport in individual carbon nanotubes by fullerene encapsulation. *Nat Mater* 2017;16:892-7. DOI PubMed
150. Fukumaru T, Fujigaya T, Nakashima N. Development of n-type cobaltocene-encapsulated carbon nanotubes with remarkable thermoelectric property. *Sci Rep* 2015;5:7951. DOI PubMed PMC
151. Aygün M, Stoppiello CT, Lebedeva MA, et al. Comparison of alkene hydrogenation in carbon nanoreactors of different diameters: probing the effects of nanoscale confinement on ruthenium nanoparticle catalysis. *J Mater Chem A* 2017;5:21467-77. DOI
152. Chamberlain TW, Earley JH, Anderson DP, Khlobystov AN, Bourne RA. Catalytic nanoreactors in continuous flow: hydrogenation inside single-walled carbon nanotubes using supercritical CO_2. *Chem Commun* 2014;50:5200-2. DOI PubMed
153. Che G, Lakshmi BB, Martin CR, Fisher ER. Metal-nanocluster-filled carbon nanotubes: catalytic properties and possible applications in electrochemical energy storage and production. *Langmuir* 1999;15:750-8. DOI
154. Ellis JE, Star A. Carbon nanotube based gas sensors toward breath analysis. *Chempluschem* 2016;81:1248-65. DOI PubMed
155. Tian R, Wang S, Hu X, et al. Novel approaches for highly selective, room-temperature gas sensors based on atomically dispersed non-precious metals. *J Mater Chem A* 2020;8:23784-94. DOI
156. Qin M, Li J, Song Y. Toward high sensitivity: perspective on colorimetric photonic crystal sensors. *Anal Chem* 2022;94:9497-507. DOI PubMed
157. Qin Z, Sun X, Zhang H, et al. A transparent, ultrastretchable and fully recyclable gelatin organohydrogel based electronic sensor with broad operating temperature. *J Mater Chem A* 2020;8:4447-56. DOI
158. Luo C, Jia J, Gong Y, Wang Z, Fu Q, Pan C. Highly sensitive, durable, and multifunctional sensor inspired by a spider. *ACS Appl Mater Interfaces* 2017;9:19955-62. DOI PubMed
159. liu H, Jiang H, Du F, Zhang D, Li Z, Zhou H. Flexible and degradable paper-based strain sensor with low cost. *ACS Sustain Chem Eng* 2017;5:10538-43. DOI
160. Kim J, Choi S, Lee J, Chung Y, Byun YT. Gas sensing properties of defect-induced single-walled carbon nanotubes. *Sens Actuator A Phys* 2016;228:688-92. DOI
161. Quang NH, Van Trinh M, Lee B, Huh J. Effect of NH_3 gas on the electrical properties of single-walled carbon nanotube bundles. *Sens Actuators B Chem* 2006;113:341-6. DOI
162. Nguyen H, Huh J. Behavior of single-walled carbon nanotube-based gas sensors at various temperatures of treatment and operation. *Sens Actuators B Chem* 2006;117:426-30. DOI
163. Qi P, Vermesh O, Grecu M, et al. Toward large arrays of multiplex functionalized carbon nanotube sensors for highly sensitive and selective molecular detection. *Nano Lett* 2003;3:347-51. DOI PubMed
164. Ramachandran K, Raj Kumar T, Babu KJ, Gnana Kumar G. Ni-Co bimetal nanowires filled multiwalled carbon nanotubes for the highly sensitive and selective non-enzymatic glucose sensor applications. *Sci Rep* 2016;6:36583. DOI PubMed PMC
165. Chimowa G, Tshabalala ZP, Akande AA, et al. Improving methane gas sensing properties of multi-walled carbon nanotubes by vanadium oxide filling. *Sens Actuators B Chem* 2017;247:11-8. DOI
166. Fedi F, Domanov O, Shiozawa H, et al. Reversible changes in the electronic structure of carbon nanotube-hybrids upon NO_2 exposure under ambient conditions. *J Mater Chem A* 2020;8:9753-9. DOI